

A unified intensity of the magnetic field in the protoplanetary disk from the Winchcombe meteorite

James F. J. BRYSON , Claire I. O. NICHOLS, and Conall MAC NIOCAILL

Department of Earth Sciences, University of Oxford, Oxford, UK

*Correspondence

James F. J. Bryson, Department of Earth Sciences, University of Oxford, South Parks Road, Oxford OX1 3AN, UK.

Email: james.bryson@earth.ox.ac.uk

(Received 14 June 2022; revision accepted 23 August 2023)

Abstract—One key feature of our protoplanetary disk that shaped its transformation into a system of planetary bodies was its vast magnetic field. Unique constraints on the properties of this field can be gleaned from paleomagnetic measurements of certain meteorites. Here, we apply this approach to the recent CM chondrite fall Winchcombe with the aim of constructing the most complete and reliable record to date of the behavior of the disk field in the outer solar system. We find that the interior of Winchcombe carries a stable, pre-terrestrial magnetization that likely dates from the period of aqueous alteration of the CM chondrite parent body. This remanence corresponds to a paleointensity of $31 \pm 17 \mu\text{T}$ accounting for the average effect of parent body rotation. Winchcombe is rich in framboids and plaquettes of magnetite, which formed via precipitation following the dissolution of iron sulfide. This contrasts with most other CM chondrites, where magnetite formed predominantly via pseudomorphic replacement of FeNi metal. Accounting for the potential differences in recording fidelities of these types of magnetite, we find that the reported paleointensities from all CM chondrites to date are likely underestimates of the disk field intensity in the outer solar system, and use our measurements to calculate a unified intensity estimate of $\sim 78 \mu\text{T}$. This paleointensity is consistent with two independent values from recent studies, which collectively argue that the disk field could have played a larger role in shaping the behavior of the disk in the outer solar system than previously considered.

INTRODUCTION

During the first ~ 5 Myr following the ignition of the Sun, our solar system transformed from a chaotic protoplanetary disk of dust and gas into an organized collection of planets, asteroids, and comets. Several features governed this transition and the properties of the bodies that formed, one of which was the vast magnetic field that threaded the disk (Wardle, 2007). Specifically, this field was able to influence the dynamics of dust and gas throughout the disk (e.g., extent of turbulence; transport rate of mass and angular momentum; Weiss et al., 2021), so had the potential to shape the rates and mechanisms by which the first planetary bodies formed (Johansen et al., 2014, 2015) and subsequently grew (Johansen & Lambrechts, 2017). As such, the disk field

potentially played several key roles throughout the hierarchy of planet building.

Unique constraints on the properties (e.g., intensity, directional stability) of this ancient field can be obtained by measuring the magnetic remanences carried by bulk meteorites and their components that recorded magnetizations during the disk's lifetime (Weiss et al., 2021). For instance, the remanences carried by individual chondrules indicate that the instantaneous intensity of the disk field was $\sim 50 \mu\text{T}$ in the noncarbonaceous (NC) reservoir (i.e., closer to the Sun; Fu et al., 2014) and $\sim 100 \mu\text{T}$ in the carbonaceous (CC) reservoir (i.e., further from the Sun; Borlina et al., 2021; Fu et al., 2021). The difference in these values has been proposed to reflect the presence of a substructure in our disk that acted as a barrier and created separate reservoirs that appear to

have exhibited distinct magnetic (and possibly dynamic) behaviors (Borlina et al., 2021; Fu et al., 2021). This finding reinforces observations from a wide range of isotopic compositions of meteorites (Bermingham et al., 2020; Kleine et al., 2020) that indicate that our solar system exhibited a rich and complex early evolution.

Another group of meteorites that has been proposed to have recorded the disk field is the CM chondrites (Bryson et al., 2019; Cournède et al., 2015). These meteorites are archetypal low-temperature, aqueously altered chondrites that consist of a suite of phases that formed on their parent asteroid through a series of reactions between primary minerals and water (Suttle et al., 2021). Two such reactions include the pseudomorphic replacement of FeNi metal to form magnetite (Palmer & Lauretta, 2011; Rubin et al., 2007; Sridhar et al., 2021) and the transformation of troilite to pyrrhotite (Schrader et al., 2021; Suttle et al., 2021). Accretion and aqueous alteration of the CM chondrite parent body have been dated to have occurred within the likely lifetime of the disk (Doyle et al., 2015; Fujiya et al., 2012; Wang et al., 2017), such that these two magnetic products could feasibly have recorded chemical remanent magnetizations (CRMs) of the disk field as they formed. Previous paleomagnetic measurements of CM chondrites have identified unidirectional remanences carried predominantly by pyrrhotite that correspond to a paleointensity of $4 \pm 3 \mu\text{T}$ (Cournède et al., 2015), which has been argued to be this CRM (Bryson et al., 2019). The sizeable difference between this value and those recorded by individual chondrules has been proposed to reflect the CM chondrites recording a time average of the variations in the disk field over the long period of aqueous alteration relative to chondrule cooling (Bryson, Weiss, Lima, et al., 2020; Cournède et al., 2015). These meteorites could, therefore, provide a unique and complementary perspective of the magnetic behavior of our disk that would help to unlock as complete an understanding as possible of this feature.

Despite this potential, the accuracy of the paleointensity recovered from CM chondrites has recently been questioned because pseudomorphic replacement can generate spurious remanences (Borlina et al., 2022). Specifically, this type of reaction can lead to the remanence of a parent phase being (partially) inherited by the product (e.g., Borlina et al., 2022; Ge et al., 2021; Heider & Dunlop, 1987; Jiang et al., 2017). Because a large portion of metal in chondrites is associated with chondrules and the magnetization of these each of these spherules is randomly oriented (Borlina et al., 2021; Fu et al., 2014), any magnetite that inherits the magnetization of its parent metal would appear unmagnetized over millimeter length scales (Cournède et al., 2015). As such, pseudomorphic replacement could

readily explain the uncommon situation found in CM chondrites where only a fraction of the possible remanence carriers is magnetized, that is, the concurrent presence of a remanence in pyrrhotite and only a minor remanence in magnetite. Importantly, paleointensities are calculated by comparing this natural remanent magnetization (NRM) to laboratory remanences that are necessarily imparted to all magnetic phases (i.e., magnetite and pyrrhotite). As such, the nature of magnetite formation in CM chondrites may mean that their paleointensities are drastic underestimates of the intensity of the disk field (Borlina et al., 2022), limiting our ability to reliably adopt these values in our effort to elucidate disk evolution and planet building.

On February 28, 2021, the Winchcombe meteorite fell in the United Kingdom (Russell et al., 2023). High-resolution scanning electron microscopy (SEM) and first-order reversal curves (FORCs) demonstrate that this CM chondrite differs from most other meteorites in this group in its morphology of magnetite (King et al., 2022). Specifically, Winchcombe is rich in framboids and plaquettes of magnetite (Figure 1), which are rare in other CM chondrites but are the dominant form of magnetite in CI and some C2-ung chondrites. These exotic forms of magnetite formed through precipitation from a fluid following the dissolution of iron sulfides (Alfving et al., 2019; Greshake et al., 2005). This formation pathway has been proposed to result from a distinct fluid chemistry during aqueous alteration (possibly due to more alkaline fluids; Sridhar et al., 2021). Interestingly, precipitation represents the conventional mechanism of CRM acquisition, whereby a new magnetic mineral forms and grows through its blocking volume (Dunlop & Özdemir, 1997). As such, framboids and plaquettes of magnetite are more likely to carry reliable CRMs than grains that form through pseudomorphic replacement. Winchcombe therefore has the potential to have recorded a more accurate paleointensity of the disk field compared to other CM chondrites, so is in a unique position to provide reliable insights into the magnetic properties of the protoplanetary disk that could help to decipher a comprehensive understanding of its field.

In this study, we present the results of a suite of paleomagnetic measurements of Winchcombe with the aims of identifying the primary remanence carrier in this meteorite and determining the intensity of the ancient magnetic field it experienced to help elucidate the magnetic behavior of our protoplanetary disk.

SAMPLES AND METHODS

Winchcombe's Magnetic Mineralogy

CM chondrites consist of a suite of minerals that formed through aqueous alteration on their parent asteroid

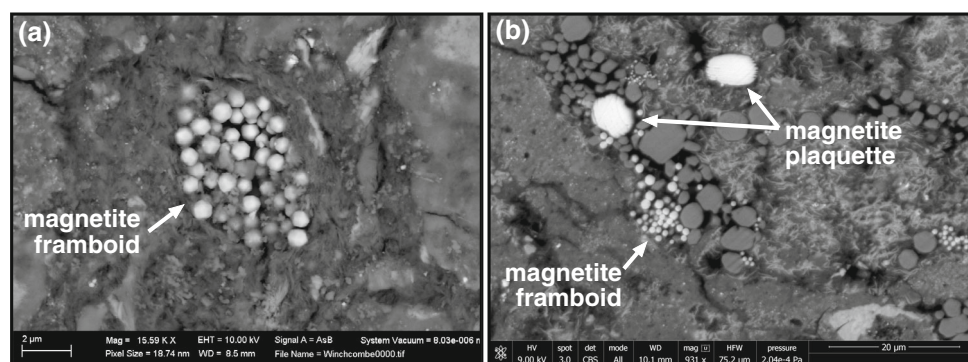


FIGURE 1. Scanning electron microscopy images of (a) framboids and (b) framboids and plaquettes of magnetite in Winchcombe.

(Rubin et al., 2007). Bulk x-ray diffraction (XRD) measurements (Howard et al., 2015) and petrographic observations (Suttle et al., 2021) indicate that this suite contains two dominant magnetic phases: magnetite and pyrrhotite. A handful of CM chondrites also contain trace amounts of metal (≤ 0.2 vol%; Howard et al., 2015). The average magnetite abundance in Winchcombe determined from XRD is 2.7 vol%, with some pieces being as rich as 6 vol% (King et al., 2022). This magnetite is found as both isolated grains that range in size from $<1 \mu\text{m}$ to $\geq 10 \mu\text{m}$ (like those found in conventional CM chondrites that form largely through pseudomorphic replacement of metal) as well as abundant framboids and plaquettes (Figure 1). FORC diagrams of two pieces of Winchcombe have been collected previously (King et al., 2022). Principal component analysis (PCA) of these diagrams indicates that $\sim 31\%$ and $\sim 58\%$ of the magnetite in these pieces exist as framboids and plaquettes with the remaining portion existing as isolated grains (Sridhar et al., 2021). XRD measurements also indicate that Winchcombe is poor in sulfides, making up only 0.6 vol% compared to ~ 1.9 vol% in typical CM chondrites (Howard et al., 2015; King et al., 2022). Moreover, petrographic observations demonstrate that the sulfide population in Winchcombe is anomalously rich in pentlandite, which is nonmagnetic (King et al., 2022). Similar to most other CM chondrites, Winchcombe does not exhibit petrographic, mineralogical, or chemical evidence that it was heated to $\geq 150^\circ\text{C}$ on its parent asteroid, arguing that it experienced a low-temperature history (King et al., 2022). As such, any measured remanence is expected to be a CRM.

Sample Preparation

An $\sim 1 \text{ cm}^3$ piece of Winchcombe (sample number BM.2022,M2-12) was provided by the Natural History Museum, London. This piece was collected from the

driveway of a house in Winchcombe, United Kingdom, on March 2, 2021. The piece has fusion crust on one face and extends $\sim 9 \text{ mm}$ into the interior of the meteorite away from this face. It originates from the same stone as most of the samples studied by King et al. (2022), including the two samples that were used to collect FORC diagrams, as well as samples that have had their magnetic mineralogy examined using SEM (Figure 1).

We cut this piece of Winchcombe into two approximately equal sized sections using a diamond wire saw lubricated with ethanediol along a plane perpendicular to the fusion crust. Each of these sections was then cut using this saw into subsamples that ranged in size from $\sim 2 \times 2 \times 2 \text{ mm}$ to $\sim 4 \times 4 \times 4 \text{ mm}$. Subsamples cut from the first section are named using letters, while subsamples cut from the second section are named using Roman numerals. We cut three fusion crust-bearing subsamples, two subsamples from within 3 mm of the visible fusion crust, and nine subsamples that originate from $\geq 3 \text{ mm}$ of this fusion crust (Table 1). We chose to include fusion-crust subsamples in our measurements because the high temperatures they reached during atmospheric entry mean they record the Earth's field immediately after the meteorite lands, so can be used to perform baked contact tests (Buchan, 2007), that is, can be used to determine whether the magnetization in the interior of Winchcombe was also affected by this field. The orientation of most of the subsamples was tracked and recorded during cutting and mounting, enabling mutually oriented remanence directions to be determined; one subsample (W_g) broke off during cutting, so was not mutually orientable with the other subsamples. As such, the remanence directions recovered from this subsample cannot be compared to those recovered from the other subsamples to perform orientation analysis, but its paleointensity can be used in the calculation of an average value.

TABLE 1. Properties of the AF demagnetization of Winchcombe.

Subsample	Mass (g)	Closest distance to visible fusion crust (mm)	NRM ($\times 10^{-3}$ $\text{Am}^2\text{kg}^{-1}$)	ARM ($\times 10^{-3}$ $\text{Am}^2\text{kg}^{-1}$)	AF range (mT)	<i>N</i>	MAD (°)	dANG (°)	Is MAD > dANG?	Dec. (°)	Inc. (°)
W_1FCa ^a											
LC	0.0513	0	12.35	—	NRM-3	3	3.2	69.7	N	269.4	48.2
MC					3–10	8	9.3	22.4	N	341.4	22.4
HC					10–85	26	4.9	19.6	N	12.8	23.9
W_1FCb ^a											
LC	0.0748	0	10.85	—	NRM-5	5	3.5	55.3	N	283.2	23.7
MC					5–12	7	9.0	16.6	N	335.4	19.8
HC					12–85	25	5.1	20.5	N	−0.6	16.8
W_1FCc ^a											
LC	0.036	0	14.19	—	NRM-5	5	7.7	33.7	N	280.3	31.7
MC					5–14	8	3.5	9.2	N	323.2	29.4
HC					14–85	24	10.2	20.4	N	321.8	59.9
W_a											
LC	0.0234	8	0.72	0.29	NRM-12	11	14.5	58.9	N	213.0	−45.0
MC					12–26	8	5.1	10.5	N	148.3	5.5
HC					26–85	18	10.4	20.0	N	143.2	28.7
W_b											
LC	0.0165	1	2.80	0.51	NRM-7	7	4.7	64.9	N	190.2	55.3
MC					7–16	7	5.2	8.4	N	323.0	39.3
HC					16–85	23	3.6	9.0	N	340.9	46.6
W_c											
LC	0.0300	1.5	3.61	0.53	NRM-5	5	2.8	16.2	N	130.4	53.9
MC					5–14	8	3.4	11.2	N	103.3	54.3
HC					14–85	24	1.5	1.0	Y	89.5	72.0
W_d											
LC	0.0368	3	1.04	0.50	NRM-9	9	7.7	83.0	N	150.4	1.3
MC					9–39	15	5.9	18.9	N	299.8	45.7
HC					39–85	13	27.6	14.9	Y	179.1	2.9
W_f											
LC	0.0881	5	0.45	0.16	NRM-5	5	16.7	42.2	N	231.4	5.2
MC					5–22	12	1.0	4.8	N	248.2	−34.7
HC					22–85	20	7.8	17.3	N	230.6	−47.5
W_g ^b											
LC	0.0172	4	1.58	0.44	NRM-8	8	4.5	17.7	N	—	—
MC					8–18	7	4.1	3.5	Y	—	—
HC					18–85	22	28.8	21.6	Y	—	—
W_i											
LC	0.0035	5	0.83	0.31	NRM-8	8	6.1	63.5	N	222.2	37.5
MC					8–16	6	16.8	52.9	N	104.2	49.8
HC					16–85	23	9.8	10.6	N	14.7	62.9
W_ii ^c											
LC	0.0042	5	0.61	0.28	NRM-9	9	7.0	10.1	N	136.5	12.5
MC					—	—	—	—	—	—	—
HC					9–85	26	26.2	7.5	Y	144.2	−2.9
W_iii											
LC	0.0048	4	0.55	0.23	NRM-6	6	8.4	48.3	N	34.7	−87.0
MC					6–12	6	8.4	11.8	N	256.0	50.1
HC					12–85	25	17.6	43.3	N	297.2	39.8

TABLE 1. *Continued.* Properties of the AF demagnetization of Winchcombe.

Subsample	Mass (g)	Closest distance to visible fusion crust (mm)	NRM ($\times 10^{-3}$ Am ² kg ⁻¹)	ARM ($\times 10^{-3}$ Am ² kg ⁻¹)	AF range (mT)	<i>N</i>	MAD (°)	dANG (°)	Is MAD > dANG?	Dec. (°)	Inc. (°)
W _{iv}											
LC	0.0068	4	0.58	0.15	NRM-7	7	5.3	55.3	N	292.1	-67.9
MC					7-26	11	6.8	10.5	N	130.5	-40.0
HC					26-85	18	29.6	20.0	Y	118.6	-10.5
W _v											
LC	0.0101	4	1.87	0.21	NRM-8	8	2.0	9.9	N	165.2	5.7
MC					8-24	10	2.7	7.3	N	163.1	17.1
HC					24-85	19	12.9	19.3	N	176.9	35.5

Abbreviations: Dec, declination; Inc, inclination; *N*: number of points.

^aFusion-crusted subsamples. ARMs not measured.

^bUnoriented subsample.

^cDoes not carry an MC component.

Demagnetization

We demagnetized the NRM carried by each subsample using alternating fields (AFs). These fields increased in peak intensity from 2 to 10 mT in steps of 1 mT, then from 10 to 30 mT in steps of 2 mT, then from 30 to 60 mT in steps of 3 mT, and finally from 60 to 85 mT in steps of 5 mT. We further demagnetized two subsamples (W_d and W_f) from 85 to 110 mT in steps of 5 mT. Each step involved applying AFs in three orthogonal directions, after which we measured the remanence remaining using a 2G Enterprises Superconducting Rock Magnetometer model 755R housed in a magnetically shielded room in the Paleomagnetism Laboratory, University of Oxford. We identified various components in the NRM by noting clear changes in direction during demagnetization and recovered each of these components using PCA (Kirschvink, 1980).

To determine paleointensities, we applied anhysteretic remanence magnetizations (ARMs) to each of the non-fusion crust-bearing subsamples after removing their NRMs, and subsequently demagnetized these remanences using the same procedure as the NRM. The ARMs had a peak AF intensity of 125 mT and a bias field of 50 μ T and were applied using an ASC Scientific D-2000 AF demagnetizer. The ancient field intensity experienced by each subsample, B_{NRM} , was determined by comparing the rate at which the NRM was lost to that at which the ARM was lost using:

$$B_{\text{NRM}} = \frac{\Delta \text{NRM}}{\Delta \text{ARM}} \frac{B_{\text{ARM}}}{f'}, \quad (1)$$

where ΔNRM and ΔARM are the changes in NRM lost and ARM lost over a given coercivity range, respectively, B_{ARM} the bias field intensity of the ARM,

and f' a calibration factor that converts ARM paleointensities to equivalent thermoremanent magnetization (TRM) values. The average value of this factor for magnetite calculated from numerous previous studies is 3.33, with a likely uncertainty of a factor between 1 and 5 (Weiss & Tikoo, 2014). We recovered paleointensities by calculating the NRM and ARM lost across each coercivity range using vector subtraction to the origin and then fitting straight lines to a plot of NRM lost against ARM lost across the same coercivity range. The errors reported on the paleointensity of each subsample correspond to the 95% uncertainty in this fitting procedure.

We chose not to perform thermal demagnetization measurements of Winchcombe for two key reasons. First, the lack of evidence that Winchcombe experienced heating to >150°C on its parent asteroid means it is not expected to carry a TRM. As such, thermal demagnetization would not represent the inverse of the process by which this rock recorded its NRM, contrasting most samples in terrestrial paleointensity studies and removing the immediate appeal to perform thermal demagnetization. Second, most meteorites acquired their mineralogy under very different conditions to those present on Earth's surface today, so are particularly prone to alteration during heating. This can lead to the destruction of magnetic phases and growth of new magnetic phases, both of which make paleointensities very difficult to determine and interpret reliably. This has been shown to be the case for other extensively aqueously altered carbonaceous chondrites with low-temperature histories (e.g., Bryson, Weiss, Lima, et al., 2020). AF techniques have previously yielded reliable paleointensities from a wide range of meteorites (Borlina et al., 2021; Bryson, Weiss, Biersteker, et al., 2020; Bryson, Weiss, Lima, et al., 2020; Cournède et al., 2015; Fu et al., 2014,

2020). As such, we focused our demagnetization efforts on AF approaches.

High-Temperature Susceptibility

Magnetic susceptibility measurements as a function of temperature were measured using an Agico MFK1 Kappa Bridge in the Nanopaleomagnetism Laboratory, University of Cambridge. These measurements were conducted with a nominal heating rate of $10^{\circ}\text{C min}^{-1}$ up to $\sim 700^{\circ}\text{C}$ while Ar gas flowed over the sample and a 200 A m^{-1} field with a frequency of 976 Hz. A total of 0.0172 g of material were measured, which was made up of a collection of small pieces that broke off during cutting from next to subsample W_f. Immediately prior to measurement, an empty sample chamber was measured to determine background values.

RESULTS

AF Demagnetization

All Winchcombe subsamples exhibit pronounced losses in their NRM as a function of increasing peak AF intensity (Figure 2a). Most subsamples cease yielding resolvable changes in NRM at peak AF intensities $\geq 50\text{ mT}$, and neither of the subsamples demagnetized to 110 mT yield measurable changes in NRM at peak AF intensities $> 85\text{ mT}$. Most of the subsamples of Winchcombe contain three components to their NRM (Figure 3; Table 1): All subsamples carry a low coercivity (LC) component (carried by grains with coercivities up to 5–12 mT depending on the subsample); all but one subsample carry a medium coercivity (MC) component (carried by grains with coercivities between 5 and 12 mT and 14–39 mT); and all subsamples carry a high coercivity (HC) component (carried by grains with coercivities between 14 and 39 mT and 85 mT).

The directions of the HC components in subsamples that originate from within 3 mm of the fusion crust (W_b and W_c) and likely two additional subsamples from deeper in the interior (W_i and W_iii) are similarly oriented to the HC components of the fusion-crusted subsamples (Figure 4a). This similarity argues that these subsamples were baked by heat from the fusion crust, so recorded (partial) TRMs of the Earth's field immediately following landing. As such, their remanences are (largely) terrestrial. The HC directions from all other subsamples differ clearly from this fusion-crusted and baked subsample direction (Figure 4), arguing that they do not carry a significant terrestrial TRM overprint. In the following, subsamples from within 3 mm of the fusion crust are referred to as “baked” (excluding the fusion-crusted subsamples themselves), while all others are referred to as “interior.”

The LC components recovered from the fusion-crusted subsamples are all similarly oriented (Figure 4a). None of the baked nor interior subsamples carry an LC component in this direction. Instead, these subsamples carry LC components that cover a wide range of directions, differing by 148° at most, in a nonsystematic pattern. These LC components typically exhibit small mean angular deviations (MADs) of $< 10^{\circ}$, which are all much smaller than their deviation angles (dANGs; Table 1). These characteristics argue that this component is almost certainly a viscous remanent magnetization (VRM) that was acquired since the meteorite fell, whereby the Earth's field has been gradually modifying a pre-existing remanence. Viscous remanences readily affect low-coercivity grains while leaving higher coercivity grains unaffected (e.g., Bryson, Weiss, Lima, et al., 2020). Winchcombe was on Earth for 14 months before we conducted our paleomagnetic measurements, during which time it will have changed orientation several times during collection, curation, shipping, and preparation, and it spent two of those months in our magnetically shielded room where a VRM could have decayed. Each subsample contains different population distributions of magnetic grains with coercivities in their LC range, so their magnetizations will each have been modified by the Earth's field to differing extents every time our parent piece of Winchcombe was reoriented, providing an explanation for the wide range and unsystematic pattern of directions recovered for this component. Similar behavior has been observed in other magnetite-rich carbonaceous chondrites (Bryson, Weiss, Biersteker, et al., 2020).

The MC components are also similarly oriented among the fusion-crusted subsamples in a different direction to that of the LC component (Figure 4b). Again, the baked and interior subsamples display a wide range of MC directions that largely differ from that of the fusion-crusted subsamples. However, unlike the LC component, the MC directions of the fusion-crusted subsamples and many of the baked and interior subsamples vary in a systematic pattern, falling on a great circle (Halls, 1976). Many of the orthogonal projections of the MC components are also particularly curved (e.g., Figure 3b,c). The MADs of most MC components are small, with all but one being less than their respective dANG, arguing that the vast majority of these components are non-origin trending. Together, these properties argue that the MC component in most subsamples is an isothermal remanent magnetization (IRM) overprint due to a static, artificial magnet acquired after Winchcombe fell. Very similar characteristics have been observed in the Paris CM chondrite, which was also concluded to carry an IRM overprint (Cournède et al., 2015). This type of remanence can alter the magnetization of low and MC grains, while leaving the magnetization of the most stable HC grains unaltered (Cournède et al., 2015), as

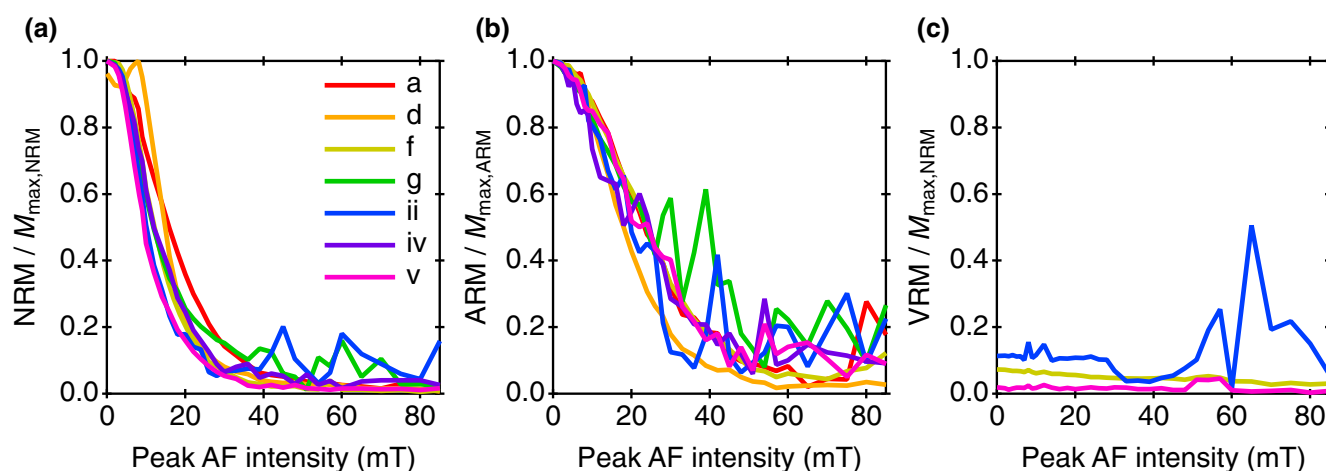


FIGURE 2. Demagnetization spectra of (a) the NRM, (b) the ARM, and (c) the VRM of non-fusion-crust, non-baked subsamples of Winchcombe as a function of peak AF intensity. The NRM and VRM spectra are normalized to the maximum value of the corresponding NRM spectra ($M_{\max,\text{NRM}}$) and each ARM spectrum is normalized to its maximum value ($M_{\max,\text{ARM}}$). (Color figure can be viewed at wileyonlinelibrary.com)

attested by the non-origin trending demagnetization of most of the MC components. Care was taken during collection and curation to minimize exposure to artificial magnets, so this overprint may have been imparted during shipping or sample preparation.

Unlike the LC and MC components, the HC components exhibit unidirectionality among most interior subsamples, which is notably differently oriented to that of the HC components of the fusion-crust and baked subsamples (Figures 3 and 4c). In all but one case, the MADs of the fusion-crust and baked subsamples do not overlap the great circle signifying the IRM overprint, arguing that these subsamples instead preserve the TRM overprint imparted by heating from the fusion crust. The difference between the HC directions of the fusion-crust and baked subsamples compared to the interior subsamples then argues that the interior subsamples were not heated appreciably by the fusion crust, so do not carry a TRM overprint of the Earth's field.

Moreover, the HC MADs of only two of the six interior subsamples overlap the great circle signifying the IRM overprint (with both these subsamples exhibiting particularly large HC MAD values). Additionally, many of the interior subsamples (e.g., Figure 3c) exhibit large differences in the directions of their MC and HC components. These two observations argue that the IRM overprint carried in the MC component cannot be the source of the HC component.

The MAD values of the HC components are larger than their respective LC and MC components, and the HC dANG values are typically smaller than the LC and MC components. The HC MAD values are greater than their respective dANG values in four non-baked interior subsamples and $<10^\circ$ less than the dANG values in

the remaining three non-baked interior subsamples, demonstrating that this component is origin trending or close to origin trending among the interior subsamples.

Taken together, these properties of the HC remanence argue that the interior of our piece of Winchcombe does not appear to have been influenced appreciably by magnetic fields on Earth and instead exhibits the characteristics expected of a remanence imparted during the early solar system.

Subsample W_i has a HC direction similar to that of the fusion-crust/baked subsamples despite originating from ~ 5 mm from the visible fusion crust. This result suggests that the fusion crust may have originally wrapped around our parent sample such that subsamples that are comparatively far from the visible fusion crust could in fact have been close enough to the surface of the parent sample to have possibly been baked. Subsample W_iii exhibits a particularly large HC dANG (43.3°) and a similar HC direction to the fusion-crust subsamples, arguing that its highest coercivity component was not accessed during our measurements and that it may carry an overprint due to baking that could make all its components difficult to distinguish. Subsamples W_i and W_iii were originally next to each other and on the outer edge of our parent piece, consistent with the hypothesis that they were closer to the original fusion crust than the other interior subsamples.

The HC directions recovered from the six oriented, non-baked interior subsamples produce a resultant vector length $R = 4.49$, indicating that the hypothesis that these directions are random can be rejected with $>99\%$ confidence (critical value, $R_{\text{crit}} = 4.48$).

Taken together, these results argue that the interior subsamples of Winchcombe carry a HC remanence that

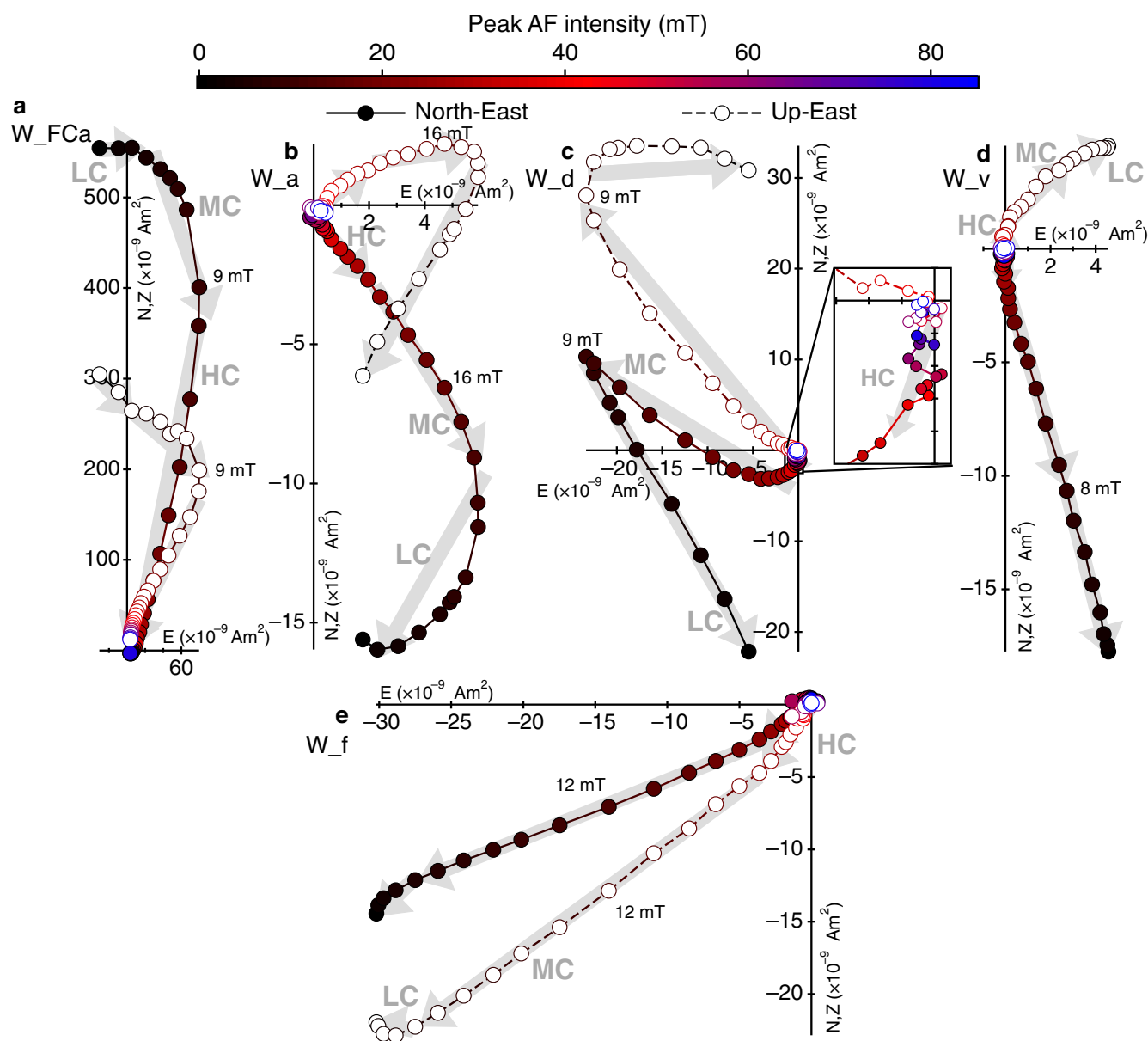


FIGURE 3. Orthogonal projection diagrams of the AF demagnetization of the NRM carried by (a) one fusion-crusted subsample and (b–e) four mutually oriented interior subsamples of Winchcombe. The LC, MC, and HC components are shown by gray arrows. Filled points represent the projection of the magnetization vector onto the north-east plane and open points represent projection onto the up-east plane. The peak AF field of each step is shown by the color. (Color figure can be viewed at [wileyonlinelibrary.com](https://onlinelibrary.wiley.com/terms-and-conditions))

has not been modified significantly since landing on Earth, so provides reliable access to Winchcombe's pre-terrestrial magnetization.

ARM Paleointensity

Paleointensities recovered using Equation (1) (Figure 5) from all three components in our non-fusion-crusted subsamples of Winchcombe are included in Table 2, and the HC paleointensities from the

seven non-fusion-crusted and non-baked subsamples are included in Figure 6.

The LC paleointensities are all large, ranging from ~ 92 to $437 \mu\text{T}$ (Table 2). Many of these values carry large uncertainties. There is no clear distinction between the LC paleointensities of baked and interior subsamples. Coupled with the wide range of directions recovered for this component among the different subsamples and the fact that it is carried by grains with particularly low coercivities, these paleointensities

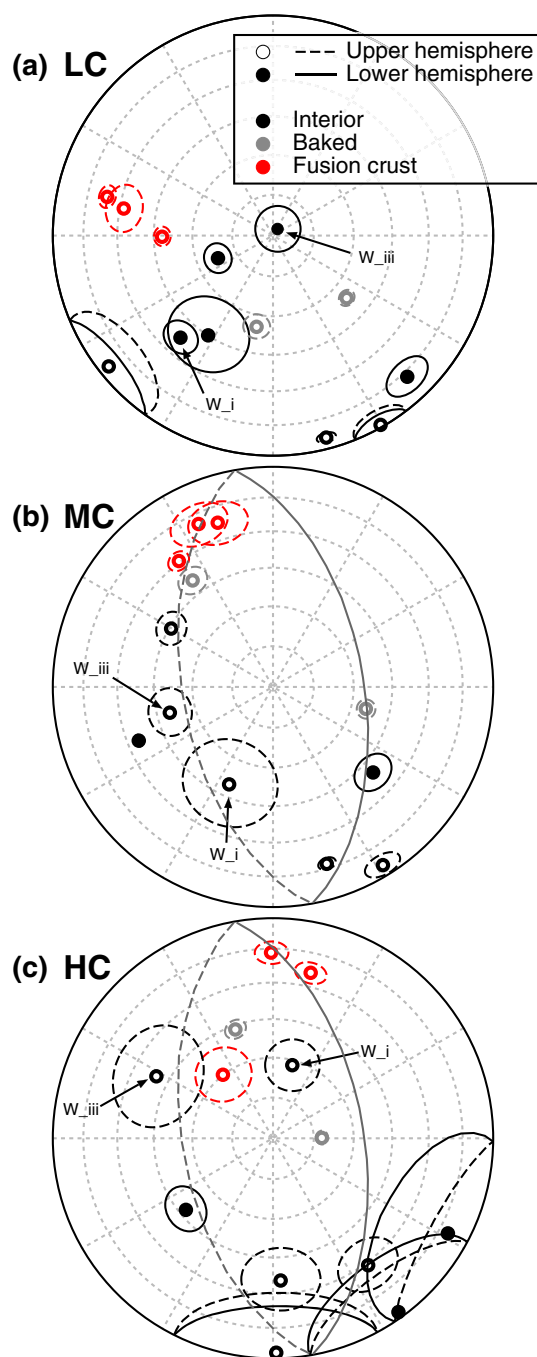


FIGURE 4. Equal area stereographic projections of the (a) LC, (b) MC, and (c) HC components of fusion crusted (red), baked (light gray), and interior (black) subsamples of Winchcombe. The MAD of each remanence is shown by the ellipse around each point. The great circle tracing the directions of the IRM overprint is shown in dark gray in (b) and (c). The two likely baked subsamples (W_i and W_{iii}) are labeled in each diagram. (Color figure can be viewed at wileyonlinelibrary.com)

indicate that the LC component is a viscous modification of the IRM overprint carried by the MC component.

The MC paleointensities are all weaker than their respective LC paleointensities, ranging from 42 to 186 mT (Table 2). These large values reinforce our deduction that the MC component is an IRM imparted since Winchcombe fell to Earth. The two baked subsamples (W_b and W_c) that originate from close to the visible fusion carry larger MC paleointensities than most other subsamples (Table 2), consistent with a magnet being placed near the surface of the sample that imparted an IRM.

The HC paleointensities are notably weaker than the LC and MC values in every subsample (Figure 6; Table 2) and exhibit a much narrower range of values (differing only by a factor of 2). Three of the baked subsamples (W_b , W_c , and W_i) yield paleointensities of $32.3 \pm 5.8 \mu\text{T}$, $50.7 \pm 5.4 \mu\text{T}$ (Figure 5a), and $58.8 \pm 13.2 \mu\text{T}$, which are very similar to that of the geomagnetic field in the UK, further supporting the HC component of the baked subsamples carrying a (near complete) terrestrial remagnetization.

Neglecting the HC components of the baked subsamples along with W_i and W_{iii} (which were very likely baked), the average HC paleointensity from the remaining seven interior subsamples is $15.5 \pm 8.5 \mu\text{T}$ (2σ ; Figure 6). The unidirectionality of the HC component over a large sample volume in a direction different to the fusion crust that does not fall along the great circle signifying the IRM overprint combined with the HC (i.e., higher stability) of these grains argues that this paleointensity is a representative pre-terrestrial value recorded by Winchcombe.

In summary, Winchcombe carries three components of magnetization. For the LC component, the particularly high paleointensities and wide range of unsystematic directions argue that this component was an IRM overprint that has since been viscously modified by the Earth's field and/or by decay during Winchcombe's time in our magnetically shielded room. For the MC component, the high paleointensities and directions that fall systematically on a great circle argue that this component reflects the original IRM overprint that has been minimally viscously modified since it was acquired. This interpretation is supported by the particularly curved nature of many of the MC demagnetizations, which has been observed previously in IRM overprints (Cournède et al., 2015). The HC component is uniformly oriented among the interior subsamples, in a notably different direction to that of the fusion crusted subsamples. Moreover, the MADs of only two of the interior subsamples fall on the great circle that signifies the IRM overprint, arguing against this as the source of the HC component. This is reinforced by the clear difference in direction between the MC and HC components in some subsamples. Together, these

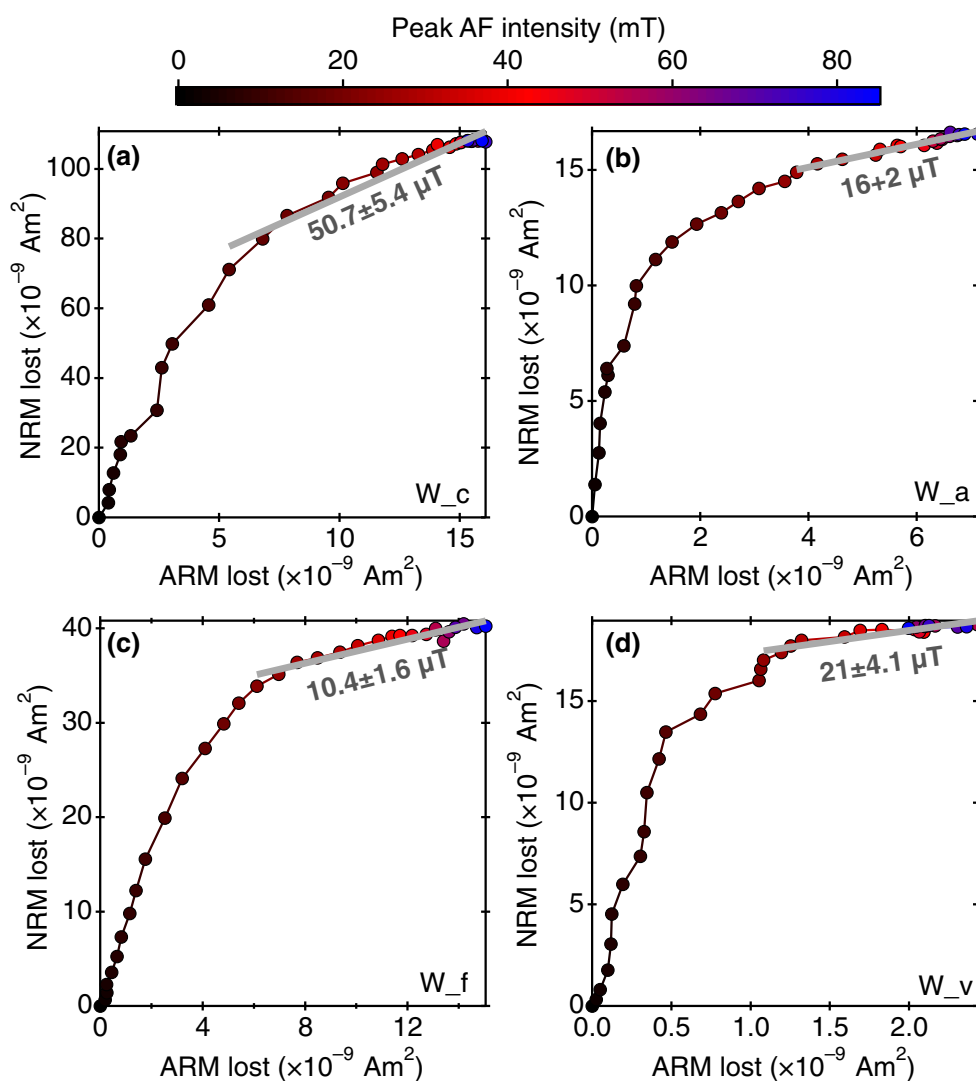


FIGURE 5. Pseudo-Arai plots, that is, NRM lost against ARM lost (50 μ T bias field), for (a) one baked subsample (W_c) and (b, c) three interior subsamples of Winchcombe (W_a , W_f , W_v). The HC paleointensity is calculated by fitting to the points across the HC range (gray line). The HC paleointensity recovered from each sample is included. The peak AF field of each point is shown by the color. (Color figure can be viewed at [wileyonlinelibrary.com](https://onlinelibrary.wiley.com/terms-and-conditions))

characteristics argue that the HC component carried by the interior subsamples is most likely pre-terrestrial. The paleointensity recovered for this component is $15.5 \pm 8.5 \mu$ T, which is appreciably weaker than the values recovered from the LC and MC components.

Demagnetization Spectra

ARM demagnetization yields a demagnetization spectrum for each subsample of Winchcombe (Figure 2b). These spectra produce mean destructive fields (MDFs) of 17–28 mT. This range is lower than that recovered from other CM chondrites of 29–56 mT (Cournède et al., 2015). This difference indicates that the assemblage of magnetic minerals in Winchcombe has a lower coercivity than that

in typical CM chondrites. This observation can be readily explained by the relative paucity of pyrrhotite in Winchcombe compared to other CM chondrites (King et al., 2022), which is a naturally higher coercivity mineral than magnetite (Roberts et al., 2006). As such, it argues that the predominant remanence carrier in Winchcombe is magnetite, in contrast to most other CM chondrites. This is consistent with the MDFs of the C2-ung chondrite WIS 91600 (Bryson, Weiss, Biersteker, et al., 2020), which also consists of abundant magnetite framboids and plaquettes. The MDFs of the NRM range from 9.5 to 16.3 mT (Figure 2a), which has likely been shifted to lower values than those recovered from the ARM by the large magnetizations carried in the LC and MC components resulting from the IRM overprint.

TABLE 2. LC, MC, and HC ARM paleointensities recovered from Winchcombe.

Subsample	LC paleointensity (μT)	LC paleointensity 2σ uncertainty (μT)	MC paleointensity (μT)	MC paleointensity 2σ uncertainty (μT)	HC paleointensity (μT)	HC paleointensity 2σ uncertainty (μT)
W_a	150.6	42.7	42.0	4.6	16.0	2.0
W_b ^a	379.8	63.1	167.9	5.9	32.3	5.8
W_c ^a	337.0	149.6	185.8	35.7	50.7	5.4
W_d	258.2	101.6	42.7	6.8	12.4	4.3
W_f	140.2	95.2	85.7	12.0	10.4	1.6
W_g	146.4	28.2	94.3	19.1	20.0	7.2
W_i ^b	141.9	66.1	78.4	24.1	58.8	13.2
W_ii	92.1	26.6	—	—	17.4	4.5
W_iii ^b	201.0	346.9	65.8	51.2	22.9	5.6
W_iv	106.9	56.1	105.0	26.5	11.3	4.5
W_v	436.7	125.0	176.4	57.3	21.0	4.1

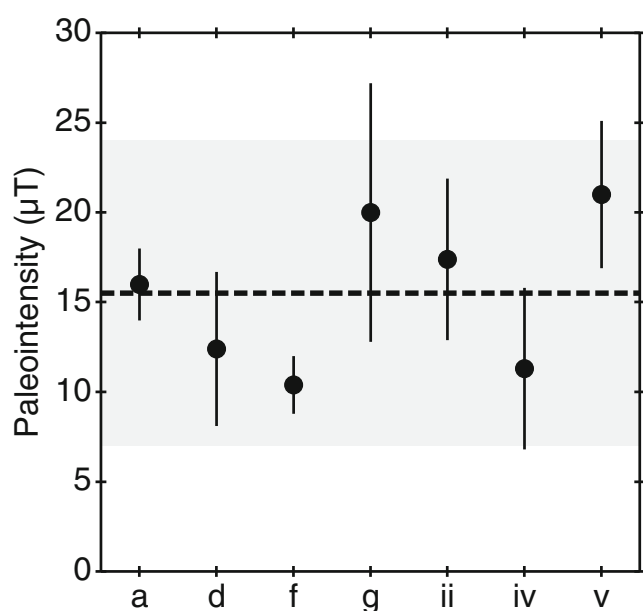
^aBaked subsamples.^bLikely baked subsamples.

FIGURE 6. Recovered HC ARM paleointensities and associated 2σ uncertainties from non-fusion-crusted and non-baked subsamples of Winchcombe. The average value ($15.5 \mu\text{T}$) and associated 2σ uncertainty ($8.5 \mu\text{T}$) of the seven individual measurements are shown by the dashed line and horizontal gray bar, respectively.

High-Temperature Susceptibility

The mass normalized magnetic susceptibility of Winchcombe during heating from room temperature to $\sim 700^\circ\text{C}$ (Figure 7) shows a minimal decrease at the pyrrhotite Curie temperature ($290\text{--}320^\circ\text{C}$) followed by a pronounced decrease at the magnetite Curie temperature (580°C). On heating above $\sim 350^\circ\text{C}$, the susceptibility gradually increases, which likely reflects alteration that creates new magnetic phases. On cooling back to room temperature, the susceptibility increases to a larger value than that measured initially, demonstrating the

production of new magnetic phases during heating. The measurements on cooling show a more pronounced change through the pyrrhotite Curie temperature than during heating, arguing that pyrrhotite was created during heating. Together, these results indicate that there is minimal pyrrhotite in the pristine sample compared to magnetite, and that alteration of the magnetic mineralogy in Winchcombe starts occurring on heating at $\sim 350^\circ\text{C}$ and creates pyrrhotite. The dominance of magnetite is consistent with the ARM demagnetization spectra (Figure 2b), further arguing that the NRM in Winchcombe is carried predominantly by this mineral, in contrast to that in most other CM chondrites. The pronounced alteration seen on heating to even low temperatures justifies our focus on AF demagnetization techniques.

VRM Demagnetization

To explore the extent to which the NRM carried by Winchcombe could have been affected by viscous remagnetization, we removed three of our interior subsamples (W_f, W_ii, and W_v) from the magnetically shielded room (after the removal of their NRM and ARM) and allowed them to acquire a viscous remanence in the Earth's field ($\sim 48 \mu\text{T}$ in Oxford) for 85.3 days. We then AF demagnetized these subsamples following the same procedure as the NRM. These measurements were performed in the Paleomagnetism Laboratory, University of Southampton. The measured rates of VRM acquisition in Tagish Lake (another meteorite that is rich in magnetite framboids and plaquettes; Bryson, Weiss, Lima, et al., 2020) argue that the difference in VRM acquisition times of Winchcombe after it fell (12 months before entering the shielded room) and during our VRM acquisition experiment introduces a small factor of only ~ 1.1 to the difference in magnitude of the VRM gained.

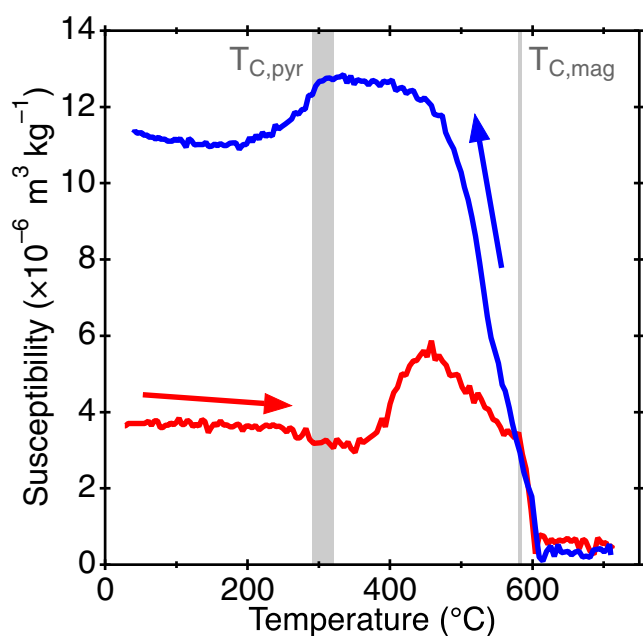


FIGURE 7. Mass normalized magnetic susceptibility of Winchcombe as a function of temperature during heating from room temperature to $\sim 700^{\circ}\text{C}$ (red), followed by cooling back to room temperature (blue). The Curie temperature of pyrrhotite ($T_{\text{C,pyr}}$) and magnetite ($T_{\text{C,mag}}$) is included as vertical gray bands. (Color figure can be viewed at [wileyonlinelibrary.com](https://onlinelibrary.wiley.com/doi/10.1111/maps.14079))

We found that these subsamples acquired VRMs with magnitudes up to only $\sim 6\%$ of the NRM, and that this VRM was effectively removed by AF fields of <10 mT in W_{ii} and W_{v} , and <30 mT in W_{v} (Figure 2c). These VRMs are much weaker than the NRM carried by these subsamples, by factors of >16 . This large difference supports our proposed IRM origin of the LC and MC components and that the MC and HC components of the NRM are not a VRM overprint. The AF fields required to remove this VRM are much lower than the respective coercivity range of the HC component of the NRM for each subsample, further arguing strongly that the HC of the NRM component is not a terrestrial VRM. The VRM acquired by Winchcombe is also notably weaker than that acquired by Tagish Lake during a similar experiment (Bryson, Weiss, Lima, et al., 2020). Together, all these traits indicate that it is extremely unlikely that the HC component we measure in Winchcombe is a VRM, consistent with its very short time of Earth before demagnetization.

DISCUSSION

The interior of Winchcombe carries a unidirectional HC remanent magnetization that is differently oriented to that of its fusion crust and IRM overprint, so appears to have been negligibly modified since arriving on Earth.

ARM measurements indicate that this HC remanence was imparted by a field with an intensity of $15.5 \pm 8.5 \mu\text{T}$.

The Stability of Winchcombe's HC Magnetization

The key controller of the stability of a meteorite's magnetic record is its magnetic mineralogy. Compared to other CM chondrites, Winchcombe is anomalously rich in framboids and plaquettes of magnetite (King et al., 2022). The grains that make up these framboids are typically 100–200 nm in size (Figure 1) and adopt vortex domain structures (Kimura et al., 2013). These properties have been shown to result in particularly stable and reliable remanence carrying capacities, with such grains being able to preserve remanences for at least the age of the solar system (Nagy et al., 2017). Because this morphology of magnetite makes up a considerable fraction of the remanence carriers in Winchcombe, the HC magnetization carried by this meteorite is likely a reliable vestige of the field recorded by this meteorite during the early solar system.

The Source of Winchcombe's HC Magnetization

Several sources of magnetic fields existed in the early solar system that could have imparted the HC remanence to Winchcombe. These include the solar wind, impacts, core dynamo activity, and the protoplanetary disk.

Based on magnetohydrodynamical modeling, the intensity of the solar wind field at the asteroid belt is predicted to have been $\ll 0.1 \mu\text{T}$ and is thought to have been amplified by factor of <3.5 ahead of an airless, asteroid-sized body (Oran et al., 2018). The weak TRMs carried by some achondrites (e.g., $<0.6 \mu\text{T}$ for volcanic angrites) corroborate this very weak field intensity of the solar wind field (Wang et al., 2017; Weiss et al., 2017). As such, the comparatively high paleointensities recovered from Winchcombe argue against the solar wind as the source of its HC magnetization.

Impacts could feasibly have generated transient magnetic fields, lasting for $\lesssim 1\text{--}10$ s on asteroid-sized bodies if they were in fact generated (Crawford & Schultz, 1999). It is plausible that this field could either impart an IRM to a meteorite or the impact could provide heat that could cause a TRM of any impact-generated field to be recorded if the meteorite cooled during the first $\lesssim 1\text{--}10$ s following an impact (Muxworthy et al., 2017). Winchcombe does not exhibit any mineralogical, structural, or chemical evidence that it was impact heated on its parent asteroid (King et al., 2022), making the latter mechanism of recording an impact-generated field particularly unlikely. The former mechanism is expected to have imparted a remanence to all the magnetic phases in a meteorite (i.e., both magnetite and pyrrhotite in a CM chondrite). Because this is not observed in CM chondrites (Cournède et al., 2015; see

The Paleointensity of Winchcombe's HC Magnetization Section), we argue that these meteorites were not magnetized by impact-generated fields. Moreover, the recovered HC paleointensity from Winchcombe is much weaker than that expected from an IRM (which is expected to be at least as strong the LC and MC paleointensities because they were imparted by the same process), further disfavoring this as the source of the HC remanence.

Based on asteroid thermal evolution modeling, core dynamo activity in these bodies has been proposed to have been delayed until >5.5 Myr after the formation of calcium-aluminum-rich inclusions (CAIs; Bryson et al., 2019; Dodds et al., 2021). The field supported by the protoplanetary disk has been proposed to have existed from the formation age of CAIs and to have dissipated by ~ 4.8 Myr after this event (Wang et al., 2017) adopting a reconciled age for the volcanic Angrites (Piralla et al., 2023). Radiometric dating of carbonates in CM chondrites argues that aqueous alteration of these meteorites occurred largely between ~ 3.5 and 5 Myr after CAI formation (Fujiya et al., 2012; Suttle et al., 2021). Both petrographic observations (Davidson, Alexander, et al., 2019; Davidson, Schrader, et al., 2019) and recent laboratory experiments (Suttle et al., 2022) indicate that magnetite (as framboids and plaquettes, as well as isolated grains) formed as one of the very first phases during the sequence of aqueous alteration, possibly starting within a few hundred days of liquid water being present. Because carbonates form at a relatively late stage during aqueous alteration of framboid- and plaquette-rich meteorites (Zolensky et al., 2002), the timing of magnetite formation almost certainly predates the ages recovered from carbonates. As such, the time of CRM acquisition in CM chondrites very likely dates from the early end of the range of recovered ages for aqueous alteration, that is, closer to ~ 3.5 Myr after CAI formation. Hence, the timing of dynamo activity compared to magnetite formation argues that the remanence carried by CM chondrites is unlikely to reflect asteroid core dynamo activity. However, it is possible that the field that threaded the disk still existed when magnetite was forming in CM chondrites, so could feasibly be the source of the remanence carried by Winchcombe.

Because all other plausible field sources can be systematically ruled out, the HC remanence in Winchcombe was most likely imparted by the disk field. This field source has also previously been proposed for other CM chondrites (Cournède et al., 2015), Allende (Fu et al., 2021), and C2-ung chondrites (Bryson, Weiss, Biersteker, et al., 2020; Bryson, Weiss, Lima, et al., 2020).

The Paleointensity of Winchcombe's HC Magnetization

The type of remanence carried by a meteorite can modify paleointensity estimates recovered from laboratory measurements. Winchcombe's thermal and aqueous history

argues that the HC component carried by this meteorite is a CRM. The efficiency with which this type of remanence records a paleointensity is uncertain (Bryson, Weiss, Lima, et al., 2020). However, McClelland (1996) found that CRMs can be within factor of ~ 1 – 2 of their equivalent TRMs for alteration over periods of $\sim 10^5$ year, similar to the duration of the various reactions that occurred during aqueous alteration (~ 10 – 10^6 year; Krot et al., 2006; Suttle et al., 2022). Moreover, Baker and Muxworthy (2023) reproduce this factor for a wide range of growth times (1 – 10^6 years) and find that growth times of $\sim 10^4$ – 10^5 years produce a value of this factor between ~ 1 and 1.4 depending on the degree of interaction between particles and the position of the peak in their coercivity distribution. These findings argue that uncertainties surrounding the recording efficiency of CRMs likely have a small impact on the paleointensities recorded during meteorite aqueous alteration. For the sake of this study and to produce values that are directly comparable to previous studies (Borlina et al., 2022; Bryson, Weiss, Biersteker, et al., 2020; Bryson, Weiss, Lima, et al., 2020; Cournède et al., 2015), we assume a factor of ~ 1 , such that the CRM paleointensity is equivalent to that of a TRM.

The paleointensity recovered from a meteorite can also be impacted by the rotation of its parent body. Based on the time scales of aqueous reactions in chondrites, we expect magnetite formation and CRM acquisition to have lasted for significantly longer than the rotation period of the CM parent asteroid (very likely <100 h). This rotation causes the body to have recorded a time average of the disk field projected along its spin axis with an intensity that depends critically on the tilt angle of the spin axis away from the field lines (Fu et al., 2014). Although the specific tilt angle of the CM parent body is unknown, the average value of this angle assuming a uniform distribution of possible spin axes over the surface of a sphere is 60° , indicating that the recorded field intensity is most likely half that of the background field. As such, the intensity of the disk field recovered from Winchcombe is most likely $31 \pm 17 \mu\text{T}$.

Winchcombe's Paleointensity Compared to that of Other CM Chondrites

The pre-terrestrial paleointensity recorded by five CM chondrites has been reported previously by Cournède et al. (2015). The average value recovered from these meteorites is $4 \pm 3 \mu\text{T}$ accounting for the average effect of parent body rotation. Thermal demagnetization measurements find only minor changes in magnetization at $>320^\circ\text{C}$ in most CM chondrites (only Murchison displays a major component of its remanence in this temperature range), arguing that the remanence in typical CM chondrites is carried predominately by pyrrhotite.

The paleointensity recovered from Winchcombe is therefore a factor of ~ 7.75 greater than that recovered from other CM chondrites. One possible explanation for this difference resides in the magnetic mineralogy of Winchcombe compared to that of other CM chondrites. Petrographic observations and FORC diagrams find that typical CM chondrites contain magnetite that formed predominantly through pseudomorphic replacement of metal ($\sim 85\%$ of magnetite in typical pieces of CM chondrites; Palmer & Lauretta, 2011), alongside pyrrhotite that formed from troilite, both during aqueous alteration on their parent body (Sridhar et al., 2021; Suttle et al., 2021; Figure 8a,c). Neither of these reactions correspond to conventional CRM acquisition mechanisms where a magnetic phase precipitates from solution and grows through its blocking volume (Dunlop & Ozdemir, 1997). As such, this magnetite and pyrrhotite could potentially carry spurious remanences. For instance, reactions that involve one magnetic phase pseudomorphing into another can lead to the remanence of the parent phase being (partially) inherited by the product regardless of the intensity of background field (e.g., Borlina et al., 2022; Ge et al., 2021; Heider & Dunlop, 1987; Jiang et al., 2017). If this is the case for the pseudomorphic reaction from metal to magnetite in chondrites (Borlina et al., 2022), it would be expected that magnetite in most CM chondrites would not be uniformly magnetized (Figure 8c) because the magnetization carried by different metal grains across millimeter length scales in chondrites is non-unidirectional (Borlina et al., 2021; Fu et al., 2014). As such, this magnetite would not carry a bulk remanence. This hypothesis readily explains the weak or absent remanence carried by this mineral in most CM chondrites (Cournède et al., 2015), as well as the remanences measured from magnetite-bearing CO3.0 chondrites (Borlina et al., 2022) and low-temperature CV_{OX,B} chondrites (Gattacceca et al., 2016). As such, this mechanism offers a self-consistent explanation for the magnetite remanences measured among most low-temperature carbonaceous chondrites. In contrast, the reaction that forms pyrrhotite may lead to a remanence being recorded because its parent troilite is non-magnetic, so there is no remanence to inherit (Figure 8a,c). Furthermore, Winchcombe is rich in framboids and plaquettes of magnetite that formed through precipitation following dissolution of iron sulfides (Alfing et al., 2019; Greshake et al., 2005). Because precipitation is the conventional CRM acquisition mechanism and there is no extant parent phase from which a remanence can be inherited, it is more likely that framboids and plaquettes (and other grains that form through precipitation) of magnetite recorded a CRM when they formed compared to grains that formed through pseudomorphic replacement (Figure 8b,d).

The lack of a remanence carried by magnetite that forms through pseudomorphic replacement of metal also provides an alternative interpretation of the current disk magnetic field chronology (Figure 9a). Recent measurements of individual chondrules extracted from primitive CO chondrules find that the disk field intensity at the time these solids formed (~ 2.5 Myr after CAI formation) was $\sim 101 \mu\text{T}$ (Borlina et al., 2021). Another recent study found that bulk, magnetite-bearing CO3.0 chondrites did not experience a field intensity $> 0.9 \mu\text{T}$ when their magnetite formed (Borlina et al., 2022). The CO parent body has been proposed to have accreted at ~ 2.7 Myr after CAI formation (Desch et al., 2018; Doyle et al., 2015). Petrographic observations (Davidson, Alexander, et al., 2019; Davidson, Schrader, et al., 2019) and laboratory experiments (Suttle et al., 2022) then argue that magnetite was one of the very first phases to form during aqueous alteration of these meteorites, possibly starting within hundreds of days of liquid water being present. The CO chondrite parent body likely took ~ 0.2 Myr to heat up to temperatures necessary to melt ice (Bryson et al., 2019; Doyle et al., 2015), placing magnetite formation at ~ 2.9 Myr after CAI formation. As such, these two paleointensities could argue that the disk field intensity decreased by approximately two orders of magnitude over only ~ 0.2 – 0.4 Myr (Figure 9a). However, paleomagnetic measurements of sulfides in Allende (Fu et al., 2021), chondrules from CR chondrites (Fu et al., 2020), and bulk CM chondrites (Cournède et al., 2015) produced paleointensities greater than this $0.9 \mu\text{T}$ limit at times after 2.7–2.9 Myr after CAI formation (Figure 9). One explanation for this observation is that the disk field intensity sharply decreased and increased, which would argue that this field fluctuated considerably over astronomically short time periods. A second, less contrived explanation is that magnetite that forms from pseudomorphic replacement metal does not record a reliable remanence of this field, meaning that the paleointensities recovered from bulk CO3.0 chondrites, low-temperature CV_{OX,B} chondrites, and CM chondrites are misleadingly weak.

It is possible to distinguish between these explanations by considering whether the recovered paleointensities from Winchcombe and other CM chondrites are consistent with the same field intensity that was recorded to different extents due to the different magnetic mineralogies among these meteorites (Figure 8g,h).

For the endmember case that magnetite in a typical CM chondrite was not able to record a remanence and assuming that pyrrhotite was able to record a reliable remanence (Figure 8a,c), this meteorite's NRM, N_{CM} , can be expressed as

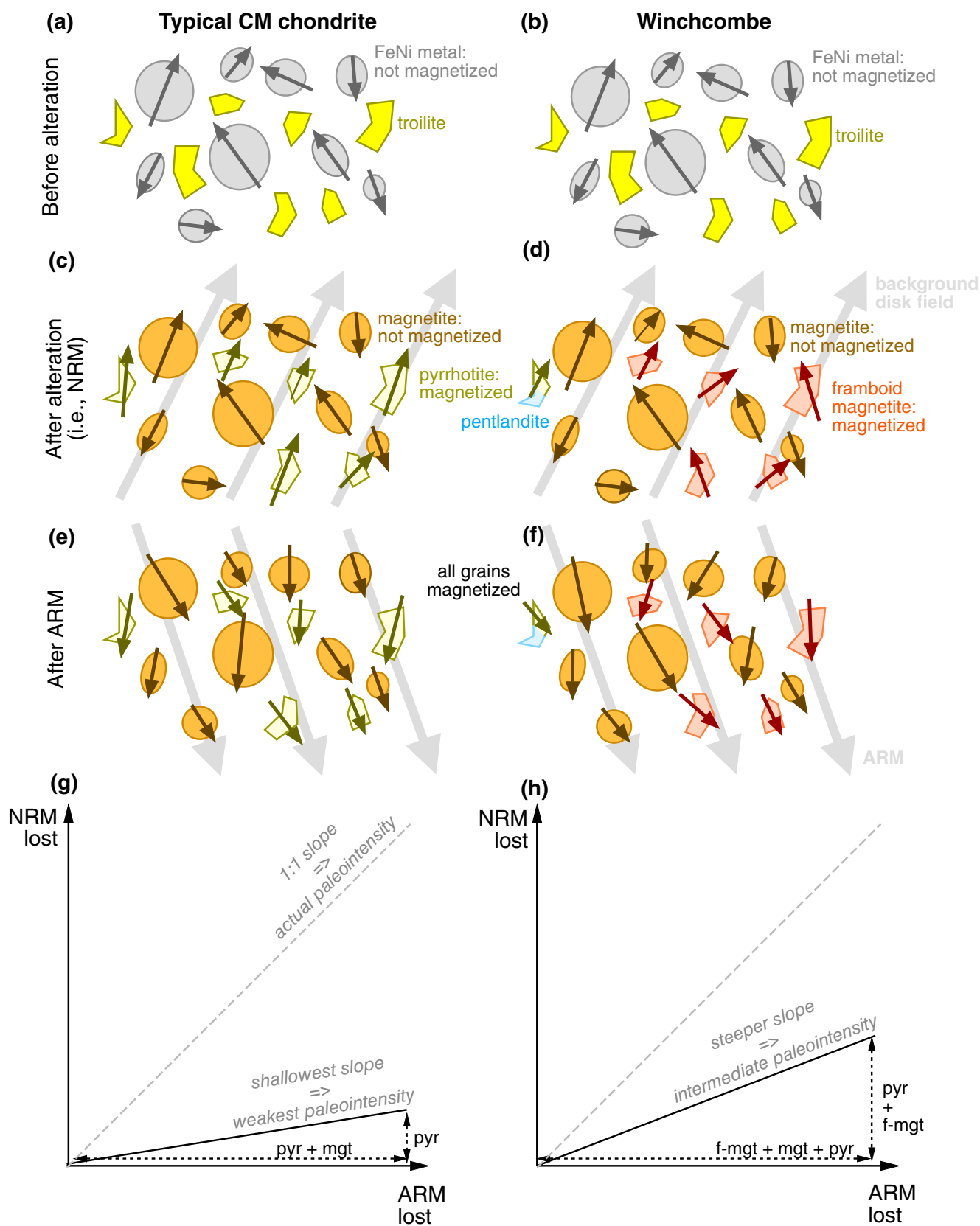


FIGURE 8. Schematic of the changes in magnetic mineralogy and magnetization (arrows) during aqueous alteration in (a, c) typical CM chondrites and (b, d) Winchcombe. Prior to alteration, grains of metal carry non-unidirectional magnetizations (Borlina et al., 2021; Fu et al., 2014). In this model, this magnetization is inherited by the magnetite that forms through pseudomorphic replacement of metal during alteration, while pyrrhotite records a new remanence with a direction biased toward the background field direction. In Winchcombe, magnetite precipitates as framboids and plaquettes following the dissolution of sulfides, which records a new remanence as it forms. (e, f) All grains are magnetized during the application of laboratory ARMs. The differences in magnetic mineralogy and remanence acquisition lead to notable differences in the magnitude of the NRM lost compared to the ARM lost (solid black line) in (g) typical CM chondrites and (h) Winchcombe. The 1:1 line that corresponds to reliable recovery of the natural field is shown by the dashed gray line. pyr: pyrrhotite; mgt: magnetite; f-mgt: framboid and plaquette magnetite. (Color figure can be viewed at [wileyonlinelibrary.com](https://onlinelibrary.wiley.com/doi/10.1111/maps.14079))

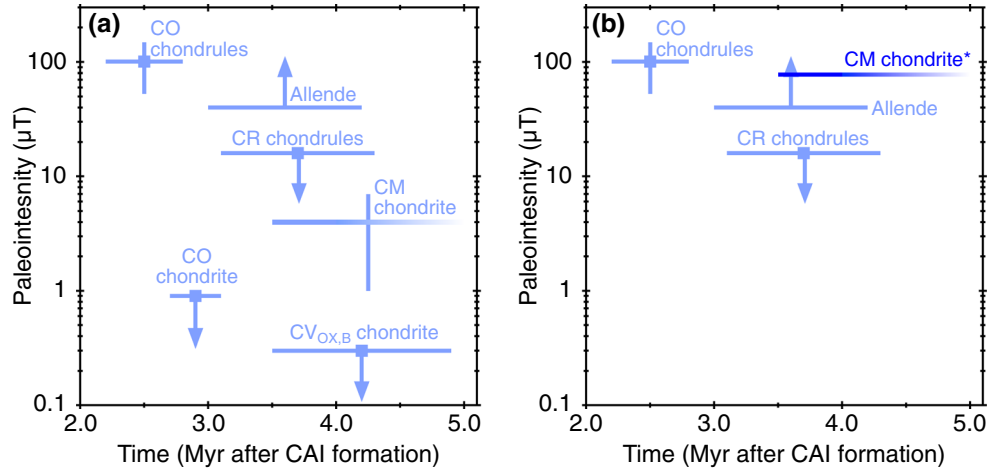


FIGURE 9. (a) Previous disk field intensity chronology in the CC reservoir constructed from paleomagnetic and radiometric dating measurements of CC chondrites and their components. Horizontal lines represent possible ranges of ages and arrows represent limits of recovered paleointensities. The change in color of the line denoting CM chondrites reflects the increased likelihood that they acquired their CRMs earlier during their period of aqueous alteration due to the quick formation of magnetite. Paleointensities and timing of CO chondrules from Borlina et al. (2021) and Kurahashi et al. (2008); Allende from Fu et al. (2021) and Carporzen et al. (2011); CR chondrules from Fu et al. (2020) and Budde et al. (2018); CM chondrites from Cournède et al. (2015) and Fujiya et al. (2012); CO chondrites from Borlina et al. (2022) and Desch et al. (2018); CV_{OX,B} chondrites (Kaba) from Gattacceca et al. (2016) and Doyle et al. (2015). (b) Unified disk field intensity record, with the new paleointensity for CM chondrites, that accounts for the findings from Winchcombe marked by the darker blue bar and “*”. The values for CO chondrites and CV_{OX,B} have been removed because their mineralogy is seemingly incapable of recording a disk field remanence in the model presented in this study. See the text for a discussion on uncertainties on the revised paleointensity for CM chondrites. (Color figure can be viewed at [wileyonlinelibrary.com](https://onlinelibrary.wiley.com/doi/10.1111/maps.14079))

$$N_{\text{CM}} = \chi_p f_{p,\text{CM}} \frac{\rho_p}{\rho_g} B, \quad (2)$$

where χ_p , ρ_p , and $f_{p,\text{CM}}$ are the susceptibility, density, and modal volume fraction in a CM chondrite of pyrrhotite, respectively; ρ_g the grain density of a CM chondrite; and B the natural field intensity. When the sample is magnetized in the laboratory (i.e., during ARM, IRM, or TRM acquisition), every magnetic grain (including magnetite) is necessarily magnetized (Figure 8e), leading to a laboratory remanence, L_{CM} ,

$$L_{\text{CM}} = \chi_p f_{p,\text{CM}} \frac{\rho_p}{\rho_g} B_L + \chi_m f_{m,\text{CM}} \frac{\rho_m}{\rho_g} B_L, \quad (3)$$

where χ_m , ρ_m , and $f_{m,\text{CM}}$ are the susceptibility, density, and modal volume fraction in a CM chondrite of magnetite, respectively, and B_L the laboratory field intensity. Hence, the paleointensity recovered from a CM chondrite, B_{CM} , can be written as

$$B_{\text{CM}} = \frac{N_{\text{CM}}}{L_{\text{CM}}} B_L = \frac{\chi_p f_{p,\text{CM}} \rho_p}{\chi_p f_{p,\text{CM}} \rho_p + \chi_m f_{m,\text{CM}} \rho_m} B. \quad (4)$$

Due to the large value of χ_m compared to χ_p (Table 3), the laboratory remanence imparted to CM chondrites would be much larger than the NRM (for equal natural and laboratory field intensities), which would have the effect of profoundly weakening the paleointensities recovered from typical CM chondrites compared to the intensity of the background field (Figure 8g). Regardless of our findings from Winchcombe, this effect will have influenced the paleointensities reported by Cournède et al. (2015) for other CM chondrites.

Assuming that frambooid and plaquette magnetite can record accurate remanences when they form (Figure 8b, d), the NRM of Winchcombe can be expressed as

$$N_W = \chi_p f_{p,W} \frac{\rho_p}{\rho_g} B + \phi \chi_m f_{m,W} \frac{\rho_m}{\rho_g} B, \quad (5)$$

where the subscript W refers to Winchcombe and ϕ is the proportion of magnetite that is in the form of frambooids and plaquettes. The laboratory magnetism of Winchcombe (Figure 8f) can be written as

$$L_W = \chi_p f_{p,W} \frac{\rho_p}{\rho_g} B_L + \chi_m f_{m,W} \frac{\rho_m}{\rho_g} B_L, \quad (6)$$

and the paleointensity recovered from Winchcombe, B_W , can be expressed as

$$B_W = \frac{N_W}{L_W} B_L = \frac{\chi_p f_{p,W} \rho_p + \phi \chi_m f_{m,W} \rho_m}{\chi_p f_{p,W} \rho_p + \chi_m f_{m,W} \rho_m} B. \quad (7)$$

The contribution from frambooid and plaquette magnetite would therefore introduce a larger change in NRM compared to that in typical CM chondrites, although this will still be less than that carried by the laboratory remanence for equal natural and laboratory field intensities. As such, Winchcombe is still expected to underestimate the natural field intensity, although less so than a typical CM chondrite (Figure 8h).

By combined Equations (4) and (7), it is then possible to express B_W as

$$B_W = \frac{\chi_p f_{p,W} \rho_p + \phi \chi_m f_{m,W} \rho_m}{\chi_p f_{p,W} \rho_p + \chi_m f_{m,W} \rho_m} \times \frac{\chi_p f_{p,CM} \rho_p + \chi_m f_{m,CM} \rho_m}{\chi_p f_{p,CM} \rho_p} \times B_{CM} \quad (8)$$

Assuming the abundance of pyrrhotite in CM chondrites matches their measured abundance of sulfides, the value of B_W for the parameters in Table 3 as a function of ϕ is shown in Figure 10a for a nominal CM chondrite paleointensity of 4 μ T. Pyrrhotite exhibits a grain size dependency to its susceptibility (Rochette et al., 2008), with the possible range in this parameter

shown by the shaded blue region and a mean value shown by the solid blue line. This calculated paleointensity agrees very well with the experimentally recovered value (horizontal orange line and shaded region) at the proportion of frambooid and plaquette magnetite determined in Winchcombe from FORC PCA (vertical gray band) reported by King et al. (2022). This finding is therefore consistent with magnetite that forms via pseudomorphic replacement from metal not being capable of recording a remanence while magnetite that forms through precipitation in the form of frambooids and plaquettes being capable of recording a remanence. It is then plausible that the range of HC paleointensities that we recover from different subsamples of Winchcombe could reflect differing abundances of frambooid and plaquette magnetite among these subsamples.

In reality, only a portion of the sulfide abundance in any CM chondrite will be pyrrhotite. This effect is particularly relevant to Winchcombe, which has an anomalously large proportion of pentlandite in its sulfide population (King et al., 2022). Fortunately, Equation (8) only depends minimally on the amount of pyrrhotite in Winchcombe, so this effect has a negligible impact on the calculated paleointensities.

Although Winchcombe seemingly cannot have recorded an accurate remanence of the disk field (Figure 8g,h), our analysis enables the paleointensity that would be recovered if all the magnetite in this meteorite was capable of having recorded a remanence (i.e., $\phi = 1$) to be estimated. This value is $\sim 78 \mu$ T for a nominal susceptibility of pyrrhotite of $35 \times 10^{-6} \text{ m}^3 \text{ kg}^{-1}$ (this paleointensity ranges from 42 to 232 μ T for the range of possible pyrrhotite susceptibilities). What's more, adopting this larger value as the input field intensity for Equation (4) yields very similar paleointensities to those recovered from typical CM chondrites ($4 \pm 3 \mu$ T) for the range of magnetite and pyrrhotite found in these meteorites (Howard et al., 2015; Figure 10b). As such, the measured paleointensities from all CM chondrites to date are consistent with this stronger disk field intensity, which was recorded to different extents due to differences in their magnetic mineralogy. This revised paleointensity is then within the error ranges of values recently recovered from other carbonaceous chondrites that recorded remanences within the disk's lifetime, namely individual CO chondrules ($101 \pm 48 \mu$ T; Borlina et al., 2021) and possibly pyrrhotite in Allende ($>40 \mu$ T, possibly $\sim 122 \mu$ T; Fu et al., 2021). As such, a time-varying disk field no longer needs to be invoked to reconcile the paleointensity recovered from CM chondrites with that recovered from chondrules and other chondrites.

This analysis demonstrates that no CM chondrite records the actual intensity of the disk field because none of these meteorites have their entire inventory of

TABLE 3. Parameters used to calculate the paleointensity recovered from CM chondrites. The abundances of pyrrhotite and magnetite in typical CM chondrites are average values from Howard et al. (2015).

Parameter	Value	Unit	Reference
χ_p	Range: 10×10^{-6} to 60×10^{-6} ; nominal value: 35×10^{-6}	$\text{m}^3 \text{kg}^{-1}$	Rochette et al. (2008)
$f_{p,\text{CM}}$	1.9	vol%	Howard et al. (2015)
$f_{p,W}$	0.6	vol%	King et al. (2022)
ρ_p	4600	kg m^{-3}	Rochette et al. (2008)
χ_m	580×10^{-6}	$\text{m}^3 \text{kg}^{-1}$	Rochette et al. (2008)
$f_{m,\text{CM}}$	1.9	vol%	Howard et al. (2015)
$f_{m,W}$	2.7	vol%	King et al. (2022)
ρ_m	5200	kg m^{-3}	Rochette et al. (2008)

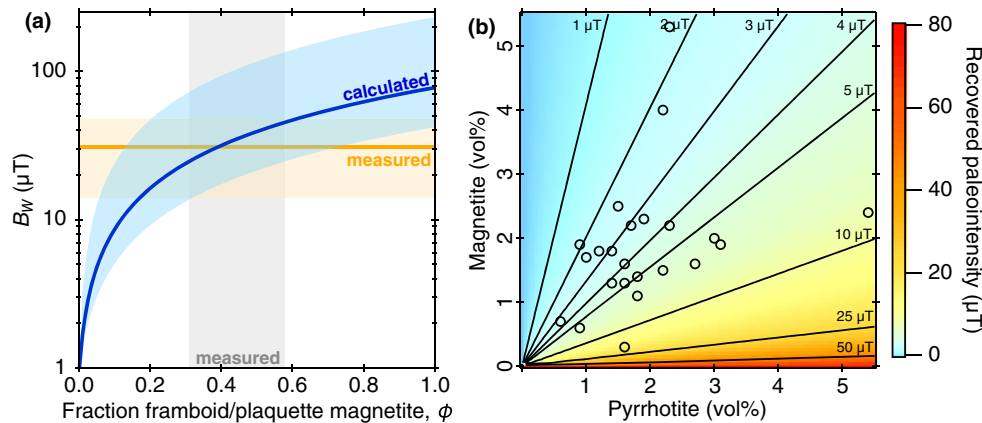


FIGURE 10. (a) Calculated paleointensity for Winchcombe (blue line and shaded region) compared to the measured value (orange line and shaded region) as a function of the fraction of framboid and plaquette magnetite in this meteorite. The range of this fraction determined from FORC PCA is shown by the vertical gray bar (King et al., 2022). The calculated paleointensity agrees well with the measured paleointensity at the measured fractions of framboid and plaquette magnetite. (b) Field intensity that would be recovered from a typical CM chondrite for the full range of magnetite and pyrrhotite volume fractions among these meteorites for a 78 μT background field (assuming no magnetite exists as framboids and plaquettes). The abundances of magnetite and pyrrhotite for the suite of CM chondrites reported by Howard et al. (2015) are included as open symbols, which almost all fall within the $4 \pm 3 \mu\text{T}$ range recovered from typical CM chondrites (Cournède et al., 2015). (Color figure can be viewed at [wileyonlinelibrary.com](https://onlinelibrary.wiley.com))

magnetite in the form of framboids and plaquettes. CI and some C2-ung chondrites have a much higher proportions of their magnetite in the form of framboids, plaquettes, and other grains that form via precipitation (up to 100%) so are much more likely to record accurate and reliable records of the disk field (Bryson, Weiss, Biersteker, et al., 2020; Bryson, Weiss, Lima, et al., 2020). If a meteorite does not contain pyrrhotite that has a composition that makes this mineral magnetic and it does not contain framboid or plaquette magnetite (or other precipitative forms), our analysis suggests it would not be capable of capturing any record of the disk field. Such a meteorite would yield paleointensities within error of 0 μT even if aqueous alteration occurred during the lifetime of the disk field. Based on magnetic susceptibility measurements (Rochette et al., 2008) and measurements

of near-stoichiometric sulfide compositions (Schrader et al., 2021), this is likely the case for CO3.0–3.2 and low-temperature CV_{OX,B} chondrites, consistent with the measured magnetic remanences of these groups (Borlina et al., 2022; Gattacceca et al., 2016). As such, we are able to present a new, reconciled record of the disk field (Figure 9b) that discounts the paleointensities recovered from CO and CV_{OX,B} chondrites and includes a stronger paleointensity recovered from CM chondrites. This new record no longer contains fluctuations in field intensity spanning several orders of magnitude, and instead indicates a strong and stable field in the CC reservoir.

In summary, the unique magnetic mineralogy of Winchcombe means it is the first bulk meteorite with paleomagnetic results that support an intense disk field in the CC reservoir, cementing this discovery in a

methodology that has been developed over decades and is widespread among the paleomagnetic community. Moreover, it provides a means of reconciling several meteorite paleomagnetic measurements made on carbonaceous chondrites over the last decade into a self-consistent model that indicates strong, stable disk field intensities in the CC reservoir. Finally, the results from Winchcombe argue that paleointensities recovered from meteorites that are expected to carry CRMs and predominantly contain magnetite that forms through pseudomorphic replacement of metal should be treated with care because they could be inaccurate by a factor of up to ~ 20 (Figure 10b) or indeed could appear unmagnetized when they may have in fact experienced a field during aqueous alteration. A thorough understanding of the changes in magnetic domain state that occur during the chemical transformation of metal into magnetite is now needed to test this model and allow as complete and reliable an understanding of the disk field as possible to be determined.

Implication of Winchcombe's Paleointensity on Disk Behavior and Evolution

Together, the results from Winchcombe alongside those from other carbonaceous chondrites are consistent with an intense, stable disk field in the CC reservoir of the protoplanetary disk. These results therefore collectively support magnetic fields potentially having played larger roles in shaping the dynamics of dust, gas, and pebbles in the CC reservoir than suggested by our previous understanding, that is, that based on the paleointensities recovered directly from typical CM chondrites (Weiss et al., 2021). Moreover, magnetohydrodynamical simulations of uniform disks (Bai, 2015; Bai & Goodman, 2009; Weiss et al., 2021) propose that their field intensities decreased monotonically by orders of magnitude over the first ~ 10 AU from the Sun. Coupled with the paleointensity for the disk field in the NC reservoir recovered from individual chondrules from Semarkona of $54 \pm 21 \mu\text{T}$ (Fu et al., 2014), the stronger field intensity argued collectively by carbonaceous chondrites challenges this model prediction. This result is consistent with our disk having been divided by a barrier into reservoirs that exhibited distinct behaviors (Borlina et al., 2021; Fu et al., 2021), supporting the findings of several isotopic measurements of meteorites (Kleine et al., 2020).

CONCLUSIONS

We conducted a suite of paleomagnetic measurements of the recent CM chondrite fall Winchcombe. We find that the interior of this meteorite carries a stable remanence with a reliable pre-terrestrial component that very likely dates

from the period of aqueous alteration on the CM chondrite parent body (~ 3.5 – 5 Myr after CAI formation). The nature of this remanence argues that it was imparted by the magnetic field supported by the protoplanetary disk. This remanence corresponds to a paleointensity of $31 \pm 17 \mu\text{T}$ accounting for the average effect of parent body rotation. This value is ~ 7.75 times larger than that recovered from other CM chondrites (Cournède et al., 2015). We find that this difference could be explained by the anomalously high abundance of framboids and plaquettes of magnetite in Winchcombe. Accounting for the possible remanence recording capabilities of the magnetic minerals and morphologies in different CM chondrites, we propose that the paleointensities recovered from this group collectively indicate a disk field intensity in the CC reservoir of $\sim 78 \mu\text{T}$. This intense value is within error of recent paleointensities recovered from individual CO chondrules (Borlina et al., 2021) and sulfides in Allende (Fu et al., 2021). Collectively, the magnetization carried by CC chondrites, therefore, argues that magnetic fields possibly played a larger role in shaping the dynamics of the CC reservoir than previously considered and support the existence of a barrier in our protoplanetary disk that introduced reservoirs with distinct behaviors.

Acknowledgments—This publication is part of the Winchcombe science team consortium, organized by the UK Fireball Alliance, and conducted by the UK Cosmochemistry Network. The authors of this paper would like to thank the UK Fireball Alliance, its constituent networks (UK Fireball Network, SCAMP, UKMON, AllSky7, NEMATODE, GMN), international collaborators (FRIPON, Global Fireball Observatory, Desert Fireball Network, University of Western Ontario and University of Helsinki), and the meteor observation camera owners who participate in the UK Fireball Alliance network for their aid in observing the fireball and helping to predict its fall position. We would also like to thank the scientists and volunteers that participated in the UK Fireball Alliance led search and recovery of the Winchcombe meteorite, and the local community, who generously reported and donated meteorite finds and enabled the team to search the strewn field. STFC are acknowledged for supporting the “Curation and Preliminary Examination of the Winchcombe Carbonaceous Chondrite Fall” project (ST/V000799/1), and Natural History Museum staff for curatorial support. The authors thank Matthew Beverly-Smith, University of Oxford, for cutting Winchcombe; Dr Richard Harrison, University of Cambridge, for collecting the high-temperature susceptibility measurements; Dr Ashley King, Natural History Museum, for collecting SEM images of magnetite in Winchcombe; and Dr Chuang Xuan and Dr Yuxi Jin,

University of Southampton, for assistance in collecting the VRM demagnetization data.

Data Availability Statement—The paleomagnetic data presented in this paper can be found on the MagIC database (<https://www2.earthref.org/MagIC>).

Editorial Handling—Prof. Adrian John Brearley

REFERENCES

- Alfing, J., Patzek, M., and Bischoff, A. 2019. Modal Abundances of Coarse-Grained (>5 μm) Components Within CI-Chondrites and their Individual Clasts—Mixing of Various Lithologies on the CI Parent Body(ies). *Geochemistry* 79: 125532.
- Bai, X.-N. 2015. Hall Effect Controlled Gas Dynamics in Protoplanetary Disks. II. Full 3D Simulations Toward the Outer Disk. *The Astrophysical Journal* 798: 84.
- Bai, X.-N., and Goodman, J. 2009. Heat and Dust in Active Layers of Protostellar Disks. *The Astrophysical Journal* 701: 737–755.
- Baker, E. B., and Muxworthy, A. R. 2023. Using Preisach Theory to Evaluate Chemical Remanent Magnetization and its Behavior During Thellier-Thellier-Coe Paleointensity Experiments. *Journal of Geophysical Research: Solid Earth* 128: e2022JB025858.
- Birmingham, K. R., Furi, E., Lodders, K., and Marty, B. 2020. The NC-CC Isotope Dichotomy: Implications for the Chemical and Isotopic Evolution of the Early Solar System. *Space Science Reviews* 216: 133.
- Borlina, C. S., Weiss, B. P., Bryson, J. F. J., and Armitage, P. J. 2022. Lifetime of the Outer Solar Nebula from Carbonaceous Chondrites. *Journal of Geophysical Research: Planets* 127: e2021JE077139.
- Borlina, C. S., Weiss, B. P., Bryson, J. F. J., Bai, X.-N., Lime, E. A., Chatterjee, N., and Mansbach, E. N. 2021. Paleomagnetic Evidence for a Disk Substructure in the Early Solar System. *Science Advances* 7: eabj6928.
- Bryson, J. F. J., Neufeld, J. A., and Nimmo, F. 2019. Constraints on Asteroid Magnetic Field Evolution and the Radii of Meteorite Parent Bodies from Thermal Modelling. *Earth and Planetary Science Letters* 521: 69–78.
- Bryson, J. F. J., Weiss, B. P., Biersteker, J. B., King, A. J., and Russell, S. S. 2020. Constraints on the Distances and Timescales of Solid Migration in the Early Solar System from Meteorite Magnetism. *The Astrophysical Journal* 896: 103.
- Bryson, J. F. J., Weiss, B. P., Lima, E. A., Gattacceca, J., and Cassata, W. 2020. Evidence for Asteroid Scattering and Distal Solar System Solids from Meteorite Paleomagnetism. *The Astrophysical Journal* 892: 126.
- Buchan, K. L. 2007. Baked Contact Test. In *Encyclopedia of Geomagnetism and Paleomagnetism*, edited by D. Gubbins, and E. Herrero-Bervera. Dordrecht: Springer. https://doi.org/10.1007/978-1-4020-4423-6_12.
- Budde, G., Kruijjer, T. S., and Kleine, T. 2018. Hf-W Chronology of CR Chondrites: Implications for the Timescales of Chondrule Formation and the Distribution of the ^{26}Al in the Solar Nebula. *Geochimica et Cosmochimica Acta* 222: 284–304.
- Carporzen, L., Weiss, B. P., Elkins-Tanton, L. T., Shuster, D. L., Ebel, D. S., and Gattacceca, J. 2011. Magnetic Evidence for a Partially Differentiated Carbonaceous Chondrite Parent Body. *Proceedings of the National Academy of Sciences of the United States of America* 108: 6386–89.
- Cournède, C., Gattacceca, J., Gounelle, M., Rochette, P., Weiss, B. P., and Zanda, B. 2015. An Early Solar System Magnetic Field Recorded in CM Chondrites. *Earth and Planetary Science Letters* 410: 62–74.
- Crawford, D. A., and Schultz, P. H. 1999. Electromagnetic Properties of Impact—Generated Plasma, Vapor and Debris. *International Journal of Impact Engineering* 23: 169–180.
- Davidson, J., Schrader, D. L., Alexander, C. M. O'D., Nittler, L. R., and Bowden, R. 2019. Re-Examining Thermal Metamorphism of the Renazzo-Like (CR) Chondrites: Insights from Pristine Miller Range 090657 and Shock-Heated Graves Nunataks 06100. *Geochimica et Cosmochimica Acta* 267: 240–256.
- Davidson, J., Alexander, C. M. O'D., Stroud, R. M., Busemann, H., and Nittler, L. R. 2019. Mineralogy and Petrology of Dominion Range 08006: A Very Primitive CO₃ Carbonaceous Chondrite. *Geochimica et Cosmochimica Acta* 265: 259–278.
- Desch, S. J., Kalyann, A., and Alexander, C. M. O'D. 2018. The Effect of Jupiter's Formation on the Distribution of Refractory Elements and Inclusions in Meteorites. *The Astrophysical Journal Supplement Series* 238: 11.
- Dodds, K. H., Bryson, J. F. J., Neufeld, J. A., and Harrison, R. J. 2021. The Thermal Evolution of Planetesimals During Accretion and Differentiation: Consequences for Dynamo Generation by Thermally-Driven Convection. *Journal of Geophysical Research: Planets* 126: e2020JE006704.
- Doyle, P. M., Jogo, K., Nagashima, K., Krot, A. N., Wakita, S., Ciesla, F. J., and Hutcheon, I. D. 2015. Early Aqueous Activity on the Ordinary and Carbonaceous Chondrite Parent Bodies Recorded by Fayalite. *Nature Communications* 6: 7444.
- Dunlop, D. J., and Ozdemir, O. 1997. *Rock Magnetism: Fundamentals and Frontiers*. Cambridge: Cambridge University Press.
- Fu, R. R., Kehayias, P., Weiss, B. P., Schrader, D. L., Bai, X.-N., and Simon, J. B. 2020. Weak Magnetic Fields in the Outer Solar Nebula Recorded in CR Chondrites. *Journal of Geophysical Research: Planets* 125: e2019E006260.
- Fu, R. R., Volk, M. W. R., Bilardello, D., Libourel, G., Lesur, G. R., and Ben Dor, O. 2021. The Fine-Scale Magnetic History of the Allende Meteorite: Implications for the Structure of the Solar Nebula. *AGU Advances* 2: e2021AV00486.
- Fu, R. R., Weiss, B. P., Lime, E. A., Harrison, R. J., Bai, X.-N., Desch, S. J., Ebel, D. S., et al. 2014. Solar Nebula Magnetic Fields Recorded in the Semarkona Meteorite. *Science* 346: 1089–92.
- Fujiya, W., Sugiura, N., Hotta, H., Ichimura, K., and Sano, Y. 2012. Evidence for the Late Formation of Hydrous Asteroids from Young Meteoritic Carbonates. *Nature Communications* 3: 627.
- Gattacceca, J., Weiss, B. P., and Gounelle, M. 2016. New Constraints on the Magnetic History of the CV Parent Body and the Solar Nebula from the Kaba Meteorite. *Earth and Planetary Science Letters* 455: 166–175.

- Ge, K., Williams, W., Nagy, L., and Tauxe, L. 2021. Models of Magnetization: Observational Evidence in Support of a Magnetic Unstable Zone. *Geochemistry, Geophysics, Geosystems* 22: e2020GC009504.
- Greshake, A., Krot, A. N., Flynn, G. J., and Keil, K. 2005. Fine-Grained Dust Rims in the Tagish Lake Carbonaceous Chondrite: Evidence for Parent Body Alteration. *Meteoritics & Planetary Science* 40: 1413–31.
- Halls, H. C. 1976. A Least-Squares Method to Find a Remanence Direction from Converging Remagnetization Circles. *Geophysical Journal International* 45: 297–304.
- Heider, F., and Dunlop, D. J. 1987. Two Types of Chemical Remanent Magnetization During the Oxidation of Magnetite. *Physics of the Earth and Planetary Interiors* 46: 24–45.
- Howard, K. T., Alexander, C. M. O'D., Schrader, D. L., and Dyl, K. A. 2015. Classification of Hydrous Meteorites (CR, CM and C2 Ungrouped) by Phyllosilicate Fraction: PSD-XRD Modal Mineralogy and Planetary Environments. *Geochimica et Cosmochimica Acta* 149: 206–222.
- Jiang, Z., Qingsong, L., Dekkers, M. J., Zhao, X., Roberts, A. P., Yang, Z., Jin, C., and Liu, J. 2017. Remagnetization Mechanisms of Triassic Red Beds from South China. *Earth and Planetary Science Letters* 479: 219–230.
- Johansen, A., Blum, J., Tanaka, H., Ormel, C., Bizzarro, M., and Rickman, H. 2014. In *The Multifaceted Planetary Formation Process, Prostars and Planets VI*, edited by H. Beuther, R. Klessen, C. Dullemond, and T. Henning. Tucson, AZ: University of Arizona Press.
- Johansen, A., and Lambrechts, M. 2017. Forming Planets Via Pebble Accretion. *Annual Review of Earth and Planetary Science* 45: 359–387.
- Johansen, A., Mac, L. M., Lacerda, P., and Bizzarro, M. 2015. Growth of Asteroids, Planetary Embryos, and Kuiper Belt Objects by Chondrule Accretion. *Science Advances* 17: e1500109.
- Kimura, Y., Sato, T., Nakamura, N., Nozawa, J., Nakamura, T., Tsukamoto, K., and Yamanoto, K. 2013. Vortex Magnetic Structure in Framboidal Magnetite Reveals Existence of Water Droplets in an Ancient Asteroid. *Nature Communications* 4: 3649.
- King, A. J., Daly, L., Rowe, J., Joy, K. H., Greenwood, R. C., Devillepoix, H. A. R., Suttle, M. D., et al. 2022. The Winchcombe Meteorite, a Unique and Pristine Witness from the Outer Solar System. *Science Advances* 8: eabq3925.
- Kirschvink, J. L. 1980. The Least-Squares Line and Plane and the Analysis of Paleomagnetic Data. *Geophysical Journal International* 62: 699–718.
- Kleine, T., Budde, G., Burkhardt, C., Kruijer, T. S., Worsham, E. A., Morbidelli, A., and Nimmo, F. 2020. The Non-Carbonaceous-Carbonaceous Meteorite Dichotomy. *Space Science Reviews* 216: 55.
- Krot, A. N., Hutcheon, I. D., Brearley, A. J., Pravdivtseva, O. V., Petaev, M. I., and Hohenberg, C. M. 2006. Timescales and Settings for Alteration of Chondritic Meteorites. In *Meteorites and the Early Solar System II*, edited by D. S. Lauretta, and H. Y. McSween, 525. Tucson, AZ: University of Arizona Press.
- Kurahashi, E., Kita, N. T., Nagahara, H., and Morishita, Y. 2008. ^{26}Al - ^{26}Mg Systematics in a Primitive CO Chondrite. *Geochimica et Cosmochimica Acta* 72: 3865–82.
- McClelland, E. 1996. Theory of CRM Acquired by Grain Growth, and its Implications for TRM Discrimination and Paleointensity Determination in Igneous Rocks. *Geophysical Journal International* 126: 271–280.
- Muxworthy, A. R., Bland, P. A., Davidson, T. M., Moore, J., Collins, G. S., and Ciesla, F. J. 2017. Evidence for an Impact-Induced Magnetic Fabric in Allende, and Exogenous Alternatives to the Core Dynamo Theory for Allende Magnetization. *Meteoritics & Planetary Science* 52: 2132–46.
- Nagy, L., Williams, W., Muxworthy, A. R., Fabian, K., Almeida, T. P., Conbhui, P. O., and Skcherbakov, V. P. 2017. Stability of Equidimensional Pseudo-Single-Domain Magnetite over Billion-Year Timescales. *Proceedings of the National Academy of Science of the United States of America* 114: 10356–60.
- Oran, R., Weiss, B. P., and Cohen, O. 2018. Were Chondrites Magnetized by the Early Solar Wind? *Earth and Planetary Science Letters* 492: 222–231.
- Palmer, E. E., and Lauretta, D. S. 2011. Aqueous Alteration of Kamacite in CM Chondrites. *Meteoritics & Planetary Science* 46: 1587–1607.
- Piralla, M., Villeneuve, J., Schnuriger, N., Bekaert, D. V., and Marrochi, Y. 2023. A Unified Chronology of Dust Formation in the Early Solar System. *Icarus* 394: 115427.
- Roberts, A. P., Liu, Q., Rowan, C. J., Chang, L., Cavallo, C., Torrent, J., and Horng, C.-S. 2006. Characterization of Hematite ($\alpha\text{-Fe}_2\text{O}_3$), Goethite ($\alpha\text{-FeOOH}$), Greigite (Fe_3S_4), and Pyrrhotite (Fe_7S_8) Using First-Order Reversal Curve Diagrams. *Journal of Geophysical Research: Solid Earth* 111: B12S35.
- Rochette, P., Gattacceca, J., Bonal, L., Bourot-Denise, M., Chevier, V., Clerc, J.-P. G., Consolmagno, G., et al. 2008. Magnetic Classification of Stony Meteorites: 2. Non-Ordinary Chondrites. *Meteoritics & Planetary Science* 43: 959–980.
- Rubin, A. E., Trigo-Rodríguez, J. M., Huber, H., and Wasson, J. T. 2007. Progressive Aqueous Alteration of CM Carbonaceous Chondrites. *Geochimica et Cosmochimica Acta* 71: 2361–82.
- Russell, S. S., King, A. J., Bates, H. C., Almeida, N. V., Greenwood, R. C., Daly, L., Joy, K. H., et al. 2023. Recovery and Curation of the Winchcombe (CM2) Meteorite. *Meteoritics & Planetary Science*. <https://doi.org/10.1111/maps.13956>.
- Schrader, D. L., Davidson, J., McCoy, T. J., Zega, T. J., Russell, S. S., Domanik, K. J., and King, A. J. 2021. The Fe/S Ratio of Pyrrhotite Group Sulfides in Chondrites: An Indicator of Oxidation and Implications for Return Samples from Asteroids Ryugu and Bennu. *Geochimica et Cosmochimica Acta* 303: 66–91.
- Sridhar, S., Bryson, J. F. J., King, A. J., and Harrison, R. J. 2021. Constraints on the Ice Composition of Carbonaceous Chondrites from their Magnetic Mineralogies. *Earth and Planetary Science Letters* 576: 117243.
- Suttle, M. D., King, A. J., Ramkissoon, N. K., Bonato, E., Franchi, I. A., Malley, J., Schofield, P. F., Najorka, J., Salge, T., and Russell, S. S. 2022. Alteration Conditions on the CM and CV Parent Bodies—Insights from Hydrothermal Experiments with the CO Chondrite Kainsaz. *Geochimica et Cosmochimica Acta* 318: 83–111.
- Suttle, M. D., King, A. J., Schofield, P. F., Bates, H., and Russell, S. S. 2021. The Aqueous Alteration of CM Chondrites, a Review. *Geochimica et Cosmochimica Acta* 299: 219–256.
- Wang, H., Weiss, B. P., Bai, X.-N., Downey, B. G., Wang, J., Wang, J., Suavet, C., Fu, R. R., and Zucolotto, M. E. 2017. Lifetime of the Solar Nebula Constrained by Meteorite Paleomagnetism. *Science* 355: 623–27.

- Wardle, M. 2007. Magnetic Fields in Protoplanetary Disks. *Astrophysics and Space Science* 311: 35–45.
- Weiss, B. P., Bai, X.-N., and Fu, R. R. 2021. History of the Solar Nebula from Meteorite Paleomagnetism. *Science Advances* 7: eaba5967.
- Weiss, B. P., and Tikoo, S. M. 2014. The Lunar Dynamo. *Science* 246: 1246753.
- Weiss, B. P., Wang, H., Sharp, T. G., Gattacceca, J., Shuster, D. L., Downey, B., Hu, J., et al. 2017. A Nonmagnetic Differentiated Early Planetary Body. *Earth and Planetary Science Letters* 468: 119–132.
- Zolensky, M. E., Nakamura, K., Gounelle, M., Mikouchi, T., Kamasa, T., Tachikawa, O., and Tinui, E. 2002. Mineralogy of Tagish Lake: An Ungrouped Type 2 Carbonaceous Chondrite. *Meteoritics & Planetary Science* 37: 737–761.
-